Influence of Discharge Gap On Material Removal and Melt Pool Movement in EDM Discharge Process

Xiaoming Yue
Shandong University
Ji Fan
Shandong University
Qi Li
Harbin Institute of Technology
Xiaodong Yang (xdyang@hit.edu.cn)
Harbin Institute of Technology
Zuoke Xu
Shandong University
Zhiyuan Chen
Shandong University

Research Article

Keywords: Electrical discharge machining (EDM), Discharge gap, Material removal, Melt pool movement, Molecular dynamics (MD) simulation

Posted Date: October 20th, 2021

DOI: https://doi.org/10.21203/rs.3.rs-973501/v1

Version of Record: A version of this preprint was published at The International Journal of Advanced Manufacturing Technology on January 28th, 2022. See the published version at https://doi.org/10.1007/s00170-021-08577-z.

Abstract

In electrical discharge machining (EDM), gap control is the key to stable processing; the discharge gap plays a significant role in EDM. To determine the influence of the discharge gap on material removal and melt pool movement, which are two fundamental issues in EDM, high-speed photography and molecular dynamics (MD) simulations were used to study the discharge process. Research results demonstrate that the discharge gap has a significant influence on material removal during the discharge process. A smaller gap width produces more and larger removed materials. The influence mechanism of the gap width on material removal is explained as follows. A smaller gap width produces discharge plasma with a smaller diameter and greater heat flux. Discharge with a greater heat flux generates more material removed during the discharge process. In addition, a smaller gap width and greater heat flux produce a stronger interaction of metal vapor jets, generating a stronger shear force acting on the melt pool. The discharge gap also influences the movement of the melt pool and the final topography of the discharge crater through external pressure acting on the melt pool. Smaller gap width produces greater external pressure acting on the melt pool, generating a bowl-shaped melt pool and a discharge crater with a depression in the center and a bulge around the edge. A larger gap width produces less external pressure acting on the melt pool, generating a flat melt pool and a discharge crater with swelling in the center and a depression around the edge.

1. Introduction

As non-conventional processing technique, EDM uses thermal energy to machine any electrically conductive material into complex precision components regardless of its hardness, rigidity, toughness, and strength. With its superior characteristics, EDM has developed rapidly in different processing methods such as sinking EDM, wire EDM, electrical arc machining (EAM),[1] micro EDM, EDM milling, and dry EDM,[2] which are widely used techniques in manufacturing, including mold manufacturing, aerospace, micro-electro mechanical systems (MEMS), and micromachining.

In EDM, the workpiece materials are erased through melting and evaporation by the plasmas in the continuous pulse discharges.[3] To ignite the discharge, the width of the discharge gap must be small (several micrometers to tens of micrometers). Unlike cutting machining, in which the tool is fed in the constant velocity, the feeding speed of the tool electrode is not constant in EDM, and the discharge gap must be controlled at a proper width by the servo feed control system.[3] If the working gap is too large, the discharge cannot be ignited; if the working gap is too small, short circuits or abnormal discharges frequently occur. Thus, the discharge gap is important in the discharge process. As EDM has a strict requirement for the gap condition, and the working gap has a substantial influence on the machining process, the discharge gap has become a research focus.

The gap width is usually approximately controlled by the servo feed control system through gap signals such as the gap voltage and current. Zhou et al. discussed the influence of servo voltage in EDM.[4] Their experiments demonstrated the machined depth was improved by almost three times using the adaptive

servo-voltage control system compared with conventional EDM. Nakagawa et al. proposed new gap control method in EDM milling to improve the machining speed.[5] Their research results indicated that using the new control method, the machining speed of the straight line and the profile were 2–6 times faster and 30% higher, respectively, compared to the conventional EDM. Many researchers have developed new servo control methods and strategies that can control the gap width more effectively to improve the EDM performance.[6, 7] Tee et al. proposed a new gap control method.[8] The research results indicated that the new gap control method improved the machining accuracy and stability of EDM. Xin et al. analyzed the discharge gap theoretically and built a mathematical model.[9] The research results verified that precise gap control can be achieved using the above mathematical model, resulting in a stable machining process. Researchers used advanced methods to control the gap width to improve EDM performance. Kunieda et al. used a piezoelectric actuator in dry EDM to decrease the incidence of short circuiting.[10] It was thought that the piezoelectric actuator could help control the gap width. Some researchers have mixed powders in the dielectric to obtain a smooth machining surface. This is known as powder-mixed EDM; the powder can increase the gap width.[11]

Fundamental research on gap width is also in progress. Li et al. studied the effect of the discharge gap in single-pulse discharge characteristics in micro-EDM.[12] The research results show that as the gap width is 40 % of the critical breakdown distance, the satisfying function can be obtained when the ignition delay and duration ratio are considered together. Takeuchi et al. investigated the debris distribution and gap width.[13] It was found that the gap width could be represented by a function of the debris concentration. Morimoto et al. studied the discharge delay time. Their research results indicated that the discharge delay time could be approximately expressed by a function of gap width.[14] Hayakawa et al. investigated machining phenomena in the EDM process using a new experimental method and device.[15] The experimental results demonstrated that the bridging of the debris distributed in the gap caused short-circuiting. They proposed a new gap control method that decreased the incidence of short-circuiting.

Many studies have been conducted on the discharge gap, yielding significant research findings. However, the influence of the discharge gap on the material removal process and melt pool movement has not been determined; these are two fundamental unsolved problems in EDM, hindering the further development of gap control methods and strategies. To determine the influence of the discharge gap on the material removal and melt pool movement during the EDM discharge process, this study uses an advanced observation mean and simulation method. Discharge experiments were conducted to compare the topography of the discharge craters obtained with different gap widths. The discharge phenomenon was directly observed by means of a high-speed camera system, and molecular dynamics (MD) simulations were used to investigate the influence mechanism of the discharge gap on material removal.

2. Experiment Of Single Pulse Discharge With Different Gap Widths

2.1 Topography of discharge crater

2.1.1 Experimental setup and details

To investigate the influence of the discharge gap on the topography of the discharge crater, the discharge was ignited with different gap widths. The experimental setup is shown in Fig. 1; the gap width is precisely controlled by an XYZ stage. It is generally difficult to ignite a discharge in an air environment with a large gap width. Thus, a compound pulsed power was applied; high-voltage pulsed power (1000 V amplitude) was used to easily ignite the discharge, and low-voltage pulsed power (100 V amplitude) provided the discharge current. As the current provided by the high-voltage pulsed power was only several milliamps, its influence on the discharge crater was neglected. The discharge conditions are presented in Table 1.

Table 1
Discharge conditions in single-pulse discharge

High voltage	**1000 V**
Low voltage	100 V
Discharge current	9 A
Gap width	10 μm, 30 μm, 60 μm, 90 μm
Tool electrode (-)	Copper rod (1 mm diameter)
Workpiece (+)	Steel block
Discharge time	200 μs

2.1.2 Experimental results and discussions

Figure 2 shows the topography of the discharge craters generated with gap widths of 10 μm (a), 30 μm (b), 60 μm (c), and 90 μm (d), measured by the laser scanning confocal microscopy (LSCM). It was observed that when the gap width was 10 μm, a discharge crater was generated with a depression in the center and a bulge around the edge. However, with a much larger gap width, the discharge craters exhibited swelling in the center and a depression around the edge. Fig. 3 shows the middle cross-section of the discharge craters generated with gap widths of 10 μm (a) and 90 μm (b). The profile change of the discharge crater is evident, and is consistent with the analysis results. Fig. 3 indicates that when the gap width is smaller, the height of the materials above the workpiece surface (colored green and labeled ‘bulge’) is much greater.

Figure 4 shows a comparison of discharge craters with different gap widths. Each experiment was repeated four times. The standard deviation error line and the average values were determined. Figure 4(a) shows the material removal volume of the discharge crater, which can be defined as the volume of the concavity subtracted from the volume of the bulge in Fig. 3. In Figure 4(a), it is found that the discharge crater generated with a gap width of 10 μm has a positive material removal volume. However, when the gap width is much larger, the material removal volume of the discharge crater becomes negative. Figure 4(b) shows the maximum depth of the discharge crater with different gap widths, which

can be measured in Fig. 3. Generally, the maximum depth of the discharge crater decreases as the gap width increases.

Experimental results indicate that the gap width has a significant influence on the discharge process. Its influence mechanism on the discharge process is investigated and discussed.

2.2 Observation of discharge process

2.2.1 Experimental setup and details

With the short depth of focus, it is generally difficult to observe most of the materials removed in the discharge process; this has been demonstrated in a previous study.[16] In this experiment, an L-shaped tool electrode was used, and the discharge was observed from the top, as shown in Figure 5 (a). Although the melt pool was completely blocked by the L-shaped tool electrode, all materials removed were easily observed as long as they were within the range of the depth of focus in the high-speed camera. Fig. 5(b) shows the experimental setup used to observe the discharge from the front. To observe the change in the diameter of the discharge plasma with different gap widths, the tool electrode contacted the workpiece and, quickly moved upward. In this process, discharge can be ignited in the air, and the diameter change of the discharge plasma can be recorded. In this device, the gap width between the anode and cathode was precisely adjusted using an XYZ motion. The working principles of the single-pulse discharge and the high-speed camera were described in our previous study.[17] Tables 2 and 3 show the experimental conditions used for observation from top and front, respectively.

Table 2. Discharge conditions for observation from top

Open voltage	110 V
Discharge current	15 A
Gap width	5 μm, 50 μm
Tool electrode (-)	Copper (0.5 mm diameter)
Workpiece (+)	Steel
Discharge time	1 ms
Dielectric	Air

Table 3. Discharge conditions for observation from front

Open voltage	150 V
Discharge current	4.2 A
Tool electrode (-)	Tungsten (1.6 mm diameter)
Workpiece (+)	Steel
Discharge time	100 ms
Dielectric	Air

2.2.2 Experimental results and discussion

Figures 6 and 7 show the discharge process from the top with gap widths of 5 μm and 50 μm, respectively, using the experimental conditions shown in Table 2. To observe the removed materials clearly, a much longer exposure time was used. The high-speed camera used an exposure time of 29 μs, an aperture of 2.8 and a frame rate of 33000 fps. The white lines in the figures represent the trajectories of the removed materials.

From Fig. 6, it was found that after the discharge was ignited, a large amount of material was removed from the electrode during the discharge process. However, Fig. 7 shows that with a gap width of 50 μm, there were no large removed materials during the discharge process; only small materials were removed occasionally. These observations verify that a smaller gap width results in more and larger material. The longer white lines shown in Fig. 6 indicate that the material removal speed was much greater with a smaller gap width.

The above experimental results raise the following questions:

(1) Why does a smaller gap width result in more removed materials in the discharge process?

(2) Why is the material removal volume positive with a smaller gap width and negative with a larger gap width?

(3) Why is a discharge crater with a depression in the center and a bulge around the edge generated with a smaller gap width, swelling in the center and a depression around the edge generated with a larger gap width?

(4) Why does the discharge crater have a greater depth and material raised higher above the workpiece surface in the discharge with a smaller gap width?

To answer these questions, the effect of the discharge gap on the material removal and melt pool movement must be determined. The discharge plasma was observed using the experimental device shown in Fig. 5(b). Images of the discharge plasma in the experimental conditions shown in Table 3 are presented in Fig. 8. The high-speed camera used an exposure time of 1.5 μs, an aperture of 4.0, and a frame rate of 22000 fps. The tool electrode contacted the workpiece surface, and quickly moved upward

for observation of the diameter change of the discharge plasma and the gap width, as shown in Fig. 8(a). The discharge plasma images show that as the gap width increases, the diameter of the discharge plasma increases. The influence mechanism of the discharge gap on material removal can be explained based on the results as the following two points.

A smaller gap width resulted in discharge plasma with a smaller diameter. With the same discharge power P (P=U×I, where U is the discharge voltage and I is the discharge current), the heat flux q (q =P/S, where S is the contact area between the discharge plasma and electrode) increased with a decrease in the plasma diameter. It was assumed that discharge with a greater heat flux q generated more removed material in the discharge process, as shown in Fig. 9. This hypothesis was verified through an MD simulation.

Our previous study proved that during the discharge process, a large number of metal vapor jets were emitted from the discharge location of the tool electrode and workpiece due to the evaporation caused by the discharge plasma.[16] These metal vapor jets collided and interacted in the gap, generating a type of shear force that acted on the melt pool and was a characteristic of material removal during the discharge process, as shown in Fig. 10(a). According to fluid mechanics theory, it was assumed that when the gap width was smaller, the interaction of the metal vapor jets was stronger and the shear force was larger, as shown in Fig. 10(b). A greater heat flux caused more evaporating materials, generating more metal vapor jets and enhancing their interaction, resulting in a greater shear force acting on the melt pool, as shown in Fig. 9. This hypothesis was verified through an MD simulation.

3. Md Simulation Of Material Removal Process With Different Gap Widths

To explain the influence mechanism of the discharge gap on material removal, two hypotheses were presented in Section 2. In this section, the discharge was studied through MD simulations to verify the hypotheses.

3.1 MD simulation model and conditions

In this study, the LAMMPS was used to achieve MD simulation of the discharge process.[18] Fig. 11(a) shows the MD model, which consists of a tool electrode and a workpiece. A discharge gap separated by the tool electrode and workpiece was defined as a vaccum for simplicity. The dimensions of the tool electrode and workpiece in the X, Y, and Z direction were 25 nm, 25 nm, and 15 nm, respectively, consisting of boundary, thermostat, and Newtonian atoms. To ensure sufficient heat conduction in the simulation model, the temperature of the thermostat atoms was maintained at 300 K during the simulation. Boundary atoms were used to prevent unexpected movement of the simulation model. Other regions of tool electrode and workpiece were Newtonian atoms, whose movement followed Newton’s law. The temperature of the simulation model was set to 300 K before the discharge process.

In the model, the workpiece and the tool electrode consisted of copper and zinc atoms, respectively. The embedded-atom method (EAM) potentials[19] and Morse potentials[20] were used to calculate the interaction forces of the copper and zinc atoms, respectively. The atomic interaction between zinc and copper materials can be described by Morse potentials.[20]

In this simulation, a circular Gaussian heat source expressed in the following equation was used to imitate the heat input from the arc column:

$P(r) = P_m \exp(-kr^2)$ (1)

here, r is the distance from the center of the arc column, P(r) is the discharge power given to an atom located at radius r, P_m is the discharge power at r = 0 and k is the heat source concentration factor.

According to the experimental results obtained by Xia,[21] the discharge energy distributed into the anode is greater than the discharge energy distributed into the cathode. Thus, P_m on the tool electrode and workpiece were assumed to be 0.1 GeV/ps and 0.12 GeV/ps, respectively, during simulation of the discharge process. The discharge time was 50 ps. After the discharge, the simulation was run for 500 ps to cool down the model. After the simulation, the material removal process was shown in the middle section of a three-dimensional model with a thickness of 1 nm ($0.5 \leq y \leq -0.5$ nm), as shown in Fig. 11(b).

3.2 Analysis of heat flux influence on material removal process

To verify the hypothesis that a heat source with a smaller diameter results in more material removed during the discharge process, MD simulations were conducted with different heat source diameters. In the MD simulation model shown in Fig. 11, only the workpiece was used; the tool electrode was deleted to prevent the influence of material removal from the tool electrode on the material removal from the workpiece. Figs. 12 and 13 show the discharge processes with heat source diameters of 16 nm and 20 nm, respectively. It is observed that with the same discharge power, a heat source with a smaller diameter generates more removed materials during the discharge process. Because the diameter of the heat source decreases with a decrease in the gap width, the heat flux of the heat source increases accordingly, resulting in more removed material from the workpiece. The diameter and depth of a discharge crater generated with a smaller heat source diameter were larger than those of a discharge crater generated with a much larger heat source diameter, as shown at t = 150 μs in Figs. 12 and 13. The final topography of the discharge craters with different heat source diameters was shown in Fig. 14, which confirms the above hypothesis.

3.3 Analysis of shear force influence on material removal process

To verify the hypothesis that a smaller gap width results in a stronger interaction of the metal vapor jets and a greater shear force, MD simulations were conducted with different gap widths. To investigate only the influence of the gap width on the shear force, the influence of the gap width on the heat source diameter was ignored in this simulation. Thus, the diameter and heat flux were assumed to be the same in simulations with different gap widths. A complete simulation model consisting of a tool electrode and a workpiece was used, as shown in Fig. 11.

Figures 15-17 show MD simulations of the discharge process with gap widths of 8 nm, 18 nm, and 28 nm, respectively. In these figures, it is found that under the action of the heat source, the materials around the discharge location were evaporated, emitting massive metal vapor jets into the gap. Because zinc has a lower boiling point than copper, much more material was emitted from the tool electrode than from the workpiece. The metal vapor jets from the tool electrode and workpiece collided in the gap and interacted, generating a shear force that acted on the melt pool, which was investigated in a previous study.[16]

Figure 15 shows that when the gap width is smaller, most of the metal vapor jets from the tool electrode and workpiece collide in the gap, generating a stronger interaction of the metal vapor jets in the gap. The interaction of the metal vapor jets was near the surface of the melt pool on the workpiece. Thus, a larger shear force acted on the melt pool, causing more materials to be removed from the melt pool. As the gap width increased, the interaction of the metal vapor jets in the gap weakened, reducing the shear force acting on the melt pool, as shown in Figure 16. Thus, the amount of material removed from the melt pool decreased. When the gap width was much larger, the interaction of the metal vapor jets occurred in the region far from the melt pool, as shown in Figure 17. As a result, the shear force caused by the interaction of the metal vapor jets, acting on the melt pool was almost negligible. Thus, little material was removed from the melt pool.

As shown at t = 150 μs in Figs. 15-17, it is also observed that both the depth and the diameter of the discharge crater decreased with an increase in the gap width, without considering the influence of the gap width on the diameter of the discharge plasma. The final topography of the discharge craters were with different gap widths was shown in Fig. 18, confirming the hypothesis that when the gap width is smaller, the interaction of the metal vapor jets is stronger and the shear force acting on the melt pool of the workpiece increases.

4. Observation Of Melt Pool Under Different Gap Widths

Figure 2 demonstrates that the discharge gap has a significant influence on the final topography of the discharge crater. To explain the influence mechanism, the influence of the discharge gap on the melt pool movement must be investigated first.

4.1 Experimental setup and method

Figure 19 shows the device used to observe the melt pool with small and large gap widths. Generally, during the discharge process, internal phenomena such as melt pool movement are completely blocked

by the discharge plasma and cannot be observed directly because the plasma emits extremely bright light. To prevent the interference of discharge plasma on the observation, a bandpass filter was used to filter out the plasma with a wavelength of 380-780 nm. Because the bandwidth of the bandpass filter was 800-820 nm, a pulsed laser source with a wavelength of 808 nm could pass through as illumination for the camera system. The working principle of this device was presented in previous research.[17] The discharge conditions are shown in Table 4.

Table 4
Discharge conditions in observation of melt pool

Voltage	**150 V**
Discharge current	5 A
Tool electrode (-)	Tungsten
Workpiece (+)	Steel

4.2 Experimental results and discussion

To determine the influence of the gap width on melt pool movement, discharge processes under different gap widths were observed. Figs. 20 and 21 show images of the melt pool using the experimental setup shown in Figure 19 with an extremely small gap width (10 μm) and a large gap width (> 200 μm), respectively. To observe the discharge process with an extremely large gap width (> 200 μm), the tool electrode contacted the workpiece and quickly moved upward. A discharge process with an extremely large gap width can be observed as the tool electrode moves upward.

Figure 20 indicates that when the gap width was 10 μm, the melt pool was bowl-shaped throughout the discharge process. The molten materials in the melt pool were pushed out, forming a depression in the center and a bulge around the edge. However, the image of the melt pool with an extremely large gap width (> 200 μm) indicates that the melt pool remained flat during most of the discharge, as shown in Figure 21. With a larger gap width, an explosion of the melt pool is more likely. The explosive process of the melt pool is shown in Figure 22. In the first frame, the melt pool remained flat. In the second frame, the melt pool started to bulge. In the third frame, the melt pool expanded to its maximum and began to explode, as shown in frames 4-8. Eventually, the melt pool became flat.

The above phenomena can be explained as follows. Based on the fluid mechanic theory, the metal vapor jets emitted from the tool electrode and workpiece collided and interacted in the gap, which can not only generate the shear force acting on the melt pool but also a discharge reaction force acting on the melt pool, which have also been verified by the experiment.[16] Then, it can be known that when the gap width was smaller, the interaction of metal vapor jets was stronger, generating higher external pressure acting on melt pool. Thus, the melt pool was pressed into a bowl under the action of higher external pressure, as shown in Figure 20. But, when the gap width was larger, the interaction of metal vapor jets was weaker, generating low external pressure acting on the melt pool. As a result, the melt pool kept flat. The influence

mechanism of the gap width on the melt pool can be explained through Figure 23. Furthermore, in the previous study, it has been demonstrated that a pressure was generated inside the melt pool during the discharge process, which made the melt pool bulge outward and served as another material removal motivity in EDM.[22] Thereby, when the gap width was much larger, under low external pressure acting on the melt pool, the melt pool could explode easily due to the action of internal pressure inside the melt pool, as shown in Figure 22.

The above analysis demonstrates that the gap width influences the melt pool movement during the discharge process through the action of external and internal pressures. Discharge craters with swelling in the center and a depression around the edge can be explained as follows. During the discharge process with a larger gap width, the external pressure caused by the interaction of the metal vapor jets was weaker; under the action of internal pressure, the melt pool tended to expand outward. When the discharge stopped, the external pressure caused by the interaction of the metal vapor jets disappeared immediately. As a result, the melt pool expanded outward and formed a discharge crater with swelling in the center and a depression around the edge. With a smaller gap width, the melt pool was pressed down and the molten materials were extruded under the action of greater external pressure, generating a discharge crater with a greater depth and material raised higher above the workpiece surface.

Fig. 24 shows the swelling formation process using the experimental setup shown in Fig. 5(b) with the discharge conditions shown in Table 2. Fig. 24(a) shows the progress of the discharge. Under the action of the discharge plasma, the melt pool did not swell. Figure 24(b) shows the discharge termination times. It is observed that after the discharge ended, the melt pool without the action of the discharge plasma was swollen and higher than the discharge in progress. After discharge, the melt pool swelled, as shown in Fig. 24(c). At the end of discharge process, the melt pool gradually cooled and formed a melting and recrystallization layer. During the expansion process of the melt pool, the volume of the melt pool increased, resulting a decrease in density. In the discharge process, tool electrode can also emit materials on the workpiece surface. Thus, the material removal volume was negative in discharges with a larger gap width, as shown in Figure 4(b).

5. Conclusions

In this study, the influence of the discharge gap on the material removal and melt pool movement during the EDM discharge process was investigated. The research results are summarized as follows:

(1) The discharge gap influences material removal during the discharge process. A smaller gap width results in more and larger removed material. The material removal speed was much greater with a smaller gap width than that with a larger gap width.

(2) The discharge gap influences the topography of the discharge crater. A discharge crater with a depression in the center and a bulge around the edge was generated with a smaller gap width. With much larger gap widths, the discharge craters exhibited swelling in the center and a depression around the edge.

(3) The influence mechanism of the gap width on material removal is explained as follows: A smaller gap width results in discharge plasma with a smaller diameter and greater heat flux. Discharge with a greater heat flux generates more removed material during the discharge process. A smaller gap width and greater heat flux produce stronger interaction of metal vapor jets, generating a stronger shear force acting on the melt pool.

(4) The discharge gap influences the movement of the melt pool during the discharge process through the action of external and internal pressures. A smaller gap width results in a greater external pressure, generating a bowl-shaped melt pool. A larger gap width produces a smaller external pressure, generating a flat melt pool.

(5) In the discharge process with a larger gap width, the external pressure caused by the interaction of the metal vapor jets was smaller; under the action of internal pressure, the melt pool tended to expand outward. When the discharge stopped, the external pressure caused by the interaction of the metal vapor jets disappeared immediately. As a result, the melt pool expanded outward and formed a discharge crater with swelling in the center and a depression around the edge.

Declarations

Funding

This work was financially supported by the National Science Foundation of China (No. 51805164, 51875133) and China Postdoctoral Science Foundation (2020M672052).

Conflicts of intrest/Competing interests

The authors declare no competing interests.

Availability of data and material

Not applicable

Code availability

Not applicable

Ethics approval

Not applicable

Consent to participate

Not applicable

Consent for publication

Not applicable

Authors' contributions

Xiaoming Yue: Conceptualization, Methodology, Investigation, Original draft preparation. Ji Fan: Data curation. Qi Li: Validation. Xiaodong Yang: Supervision, Writing-Reviewing and Editing, Funding acquisition. Zuoke Xu, Zhiyuan Chen: Software.

References

1. Zhang M, Zhang Q, Dou LY, Zhu G, Dong CJ (2016) An independent discharge status detection method and its application in EAM milling. Int J Adv Manuf Technol 87:909–918. https://doi.org/10.1007/s00170-016-8537-0
2. Kunieda M, Miyoshi Y, Takaya T, Nakajima N, Yu ZB, Yoshida M (2003) High speed 3D milling by dry EDM. Cirp Ann-Manuf Techn 52(1):147–150. DOI:10.1016/S0007-8506(07)60552-6
3. Kunieda M (2013) Electrical Discharge Machining Processes. In: Andrew YCN (ed) Handbook of Manufacturing Engineering and Technology. Springer, London, pp 1–26
4. Zhou M, Mu X, He L, Ye Q (2019) Improving EDM performance by adapting gap servo-voltage to machining state. J Manuf Process 37:101–113. DOI:10.1016/j.jmapro.2018.11.013
5. Nakagawa T, Yuzawa T, Sampei M, Hirata A (2017) Improvement in machining speed with working gap control in EDM milling. Precis Eng 47:303–310. DOI:10.1016/j.precisioneng.2016.09.004
6. Rajurkar KP, Wang WM, Lindsay RP (1989) A New Model Reference Adaptive Control of EDM. Cirp Ann-Manuf Techn 38(1):183–186. DOI:10.1016/S0007-8506(07)62680-8
7. Rajurkar KP, Wang WM, Lindsay RP (1990) Real-Time Stochastic Model and Control of EDM. Cirp Ann-Manuf Techn 39(1):187–190. DOI:10.1016/S0007-8506(07)61032-4
8. Tee KTP, Hoseinnezhad R, Brandt M, Mo J (2013) Gap width control in electrical discharge machining, using type-2 fuzzy controllers. International Conference on Control, Automation and Information Sciences (ICCAIS) 140-145. doi: 10.1109/ICCAIS.2013.6720544
9. Xin B, Gao M, Li SJ, Feng B (2020) Modeling of Interelectrode Gap in Electric Discharge Machining and Minimum Variance Self-Tuning Control of Interelectrode Gap. Math Probl Eng 2020:1–20. DOI:10.1155/2020/5652197
10. Kunieda M, Takaya T, Nakano S (2004) Improvement of dry EDM characteristics using piezoelectric actuator. Cirp Ann-Manuf Techn 53(1):183–186. DOI:10.1016/S0007-8506(07)60674-X
11. Philip JT, Mathew J, Kuriachen B (2021) Transition from EDM to PMEDM – Impact of suspended particulates in the dielectric on Ti6Al4V and other distinct material surfaces: A review. J Manuf Process 64(2):1105–1142. DOI:10.1016/j.jmapro.2021.01.056
12. Li ZK, Bai JC (2017) Impulse discharge method to investigate the influence of gap width on discharge characteristics in micro-EDM. Int J Adv Manuf Tech 90:1769–1777. DOI:10.1007/s00170-016-9508-1

13. Takeuchi H, Kunieda M (2007) Relation between Debris Concentration and Discharge Gap Width in EDM Process. Journal of The Japan Society of Electrical Machining Engineers 41(98):156–162. DOI:10.2526/jseme.41.156
14. Morimoto K, Kunieda M (2009) Sinking EDM simulation by determining discharge locations based on discharge delay time. Cirp Ann-Manuf Techn 58(1):221–224. DOI:10.1016/j.cirp.2009.03.069
15. Hayakawa S, Takahashi M, Itoigawa F, Nakamura T (2004) Study on EDM phenomena with in-process measurement of gap distance. J Mater Process Tech 149(1-3):250–255. DOI:10.1016/j.jmatprotec.2003.11.057
16. Yue XM, Yang XD, Kunieda M (2018) Influence of metal vapor jets from tool electrode on material removal of workpiece in EDM. Precis Eng 53:278–288. DOI:10.1016/j.precisioneng.2018.04.012
17. Yue XM, Yang XD, Li Q, Li XH (2020) Novel methods for high-speed observation of material removal and melt pool movement in EDM. Precis Eng 66:295–305. DOI:10.1016/j.precisioneng.2020.07.009
18. Sandia Corporation (2017) LAMMPS. http://lammps.sandia.gov/. accessed 13 November 2017
19. Foiles SM, Baskes MI, Daw MS (1986) Embedded-Atom-Method Functions for the Fcc Metals Cu, Ag, Au, Ni, Pd, Pt, and Their Alloys. Phys Rev B 33:7983–7991. DOI:10.1103/physrevb.33.7983
20. Erkoc S (1997) Empirical many-body potential energy functions used in computer simulations of condensed matter properties. Physics Reports 278(2):79–105. DOI:10.1016/S0370-1573(96)00031-2
21. Xia H, Kunieda M, Nishiwaki N (1996) Removal amount difference between anode and cathode in EDM process. International Journal of Electrical Machining 1:45–52. DOI:10.2526/jseme.28.59_31
22. Yue XM, Yang XD (2017) Molecular dynamics simulation of single pulse discharge process: clarifying the function of pressure generated inside the melting area in EDM. Mol Simulat 43(12):935–944. DOI:10.1080/08927022.2017.1306649

Figures

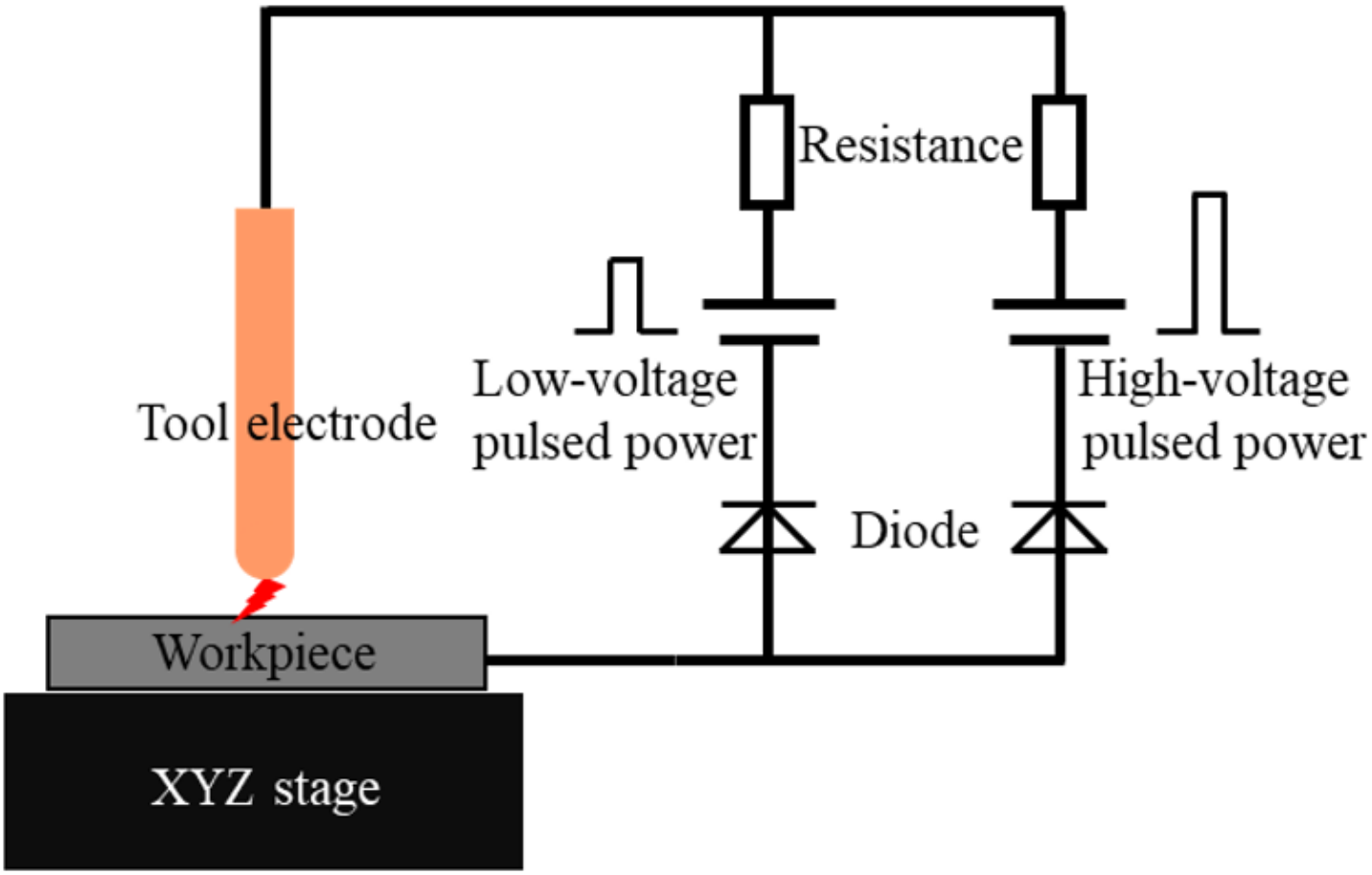

Figure 1

Diagram of single-pulse discharge

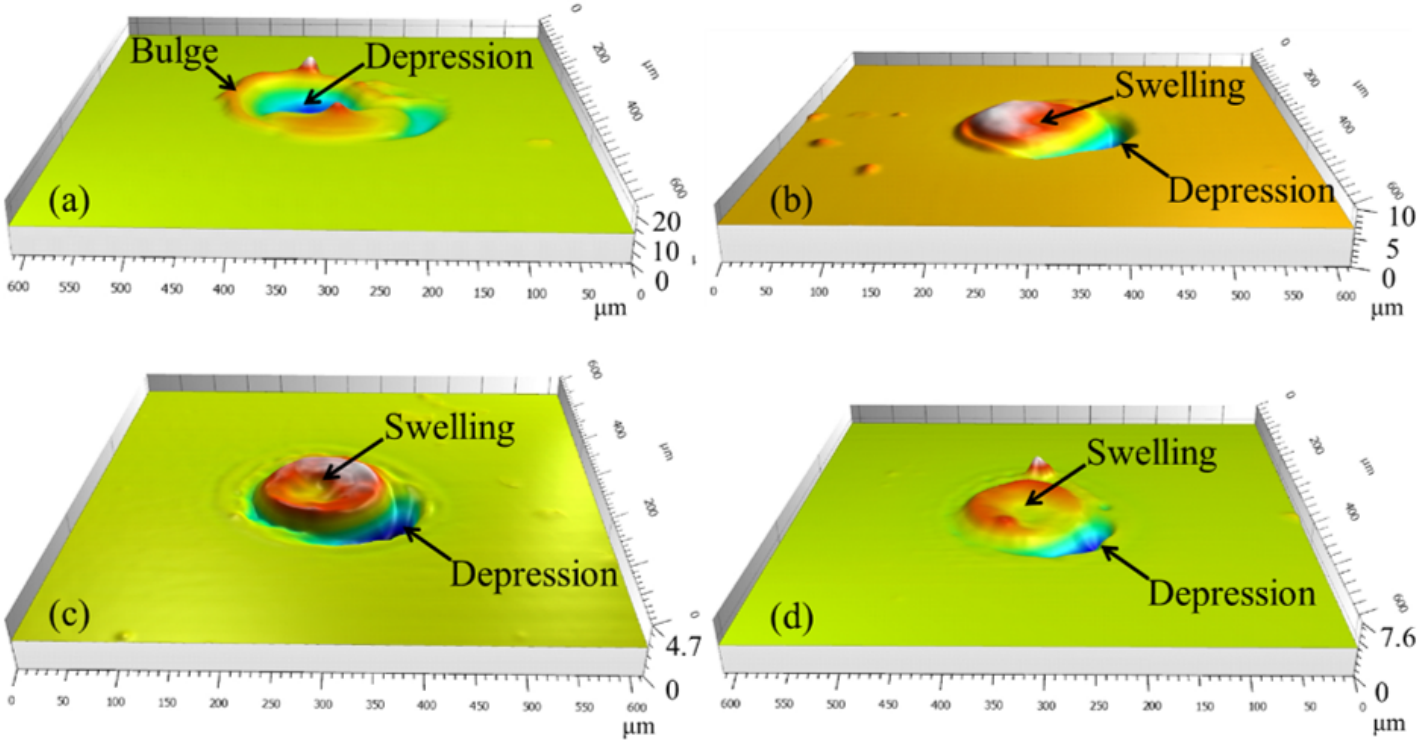

Figure 2

Topography of discharge craters generated with gap widths of (a) 10 μm; (b) 30 μm; (c) 60 μm; (d) 90 μm

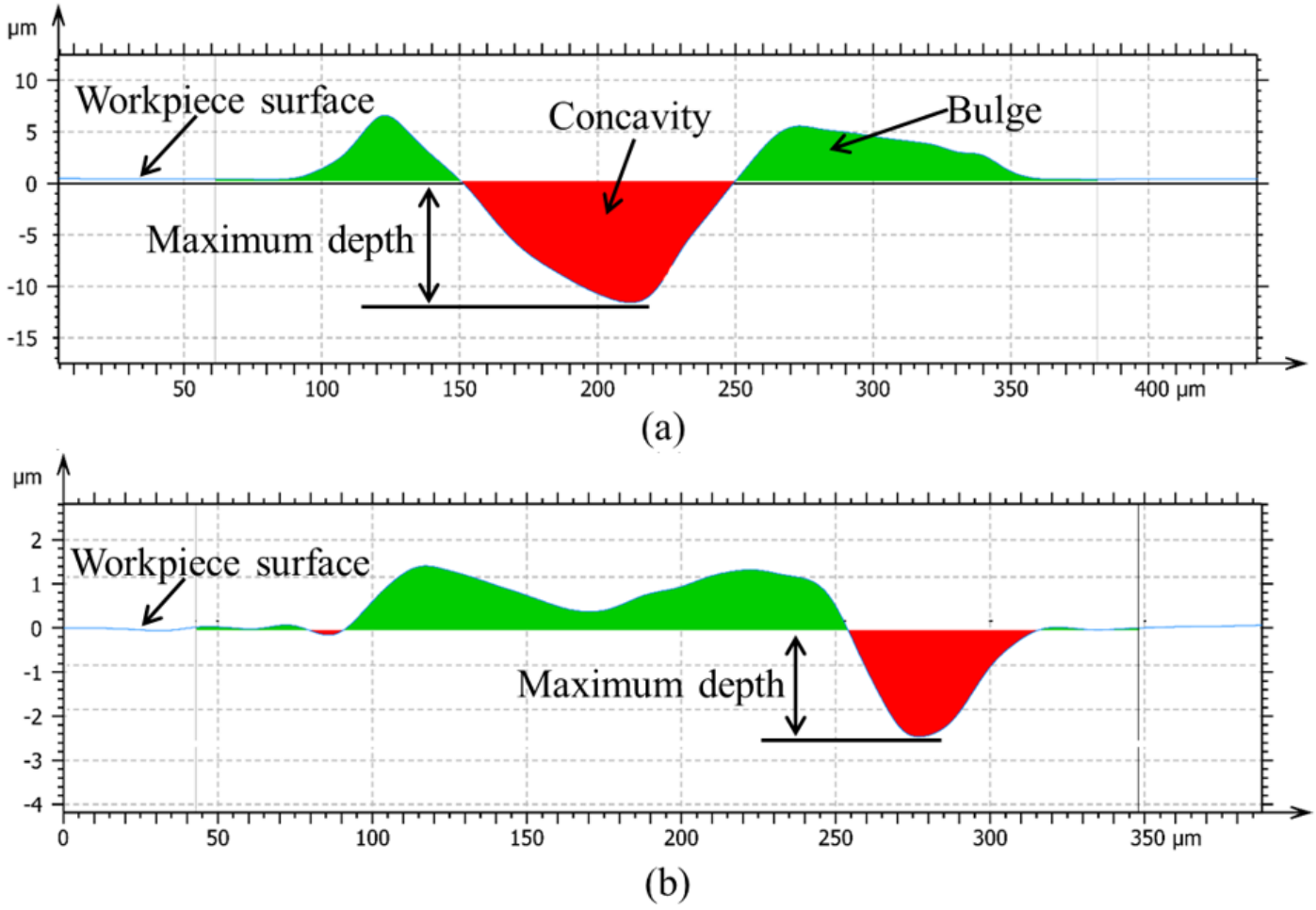

Figure 3

Middle cross-section of discharge craters generated with gap widths of (a) 10 μm and (b) 90 μm

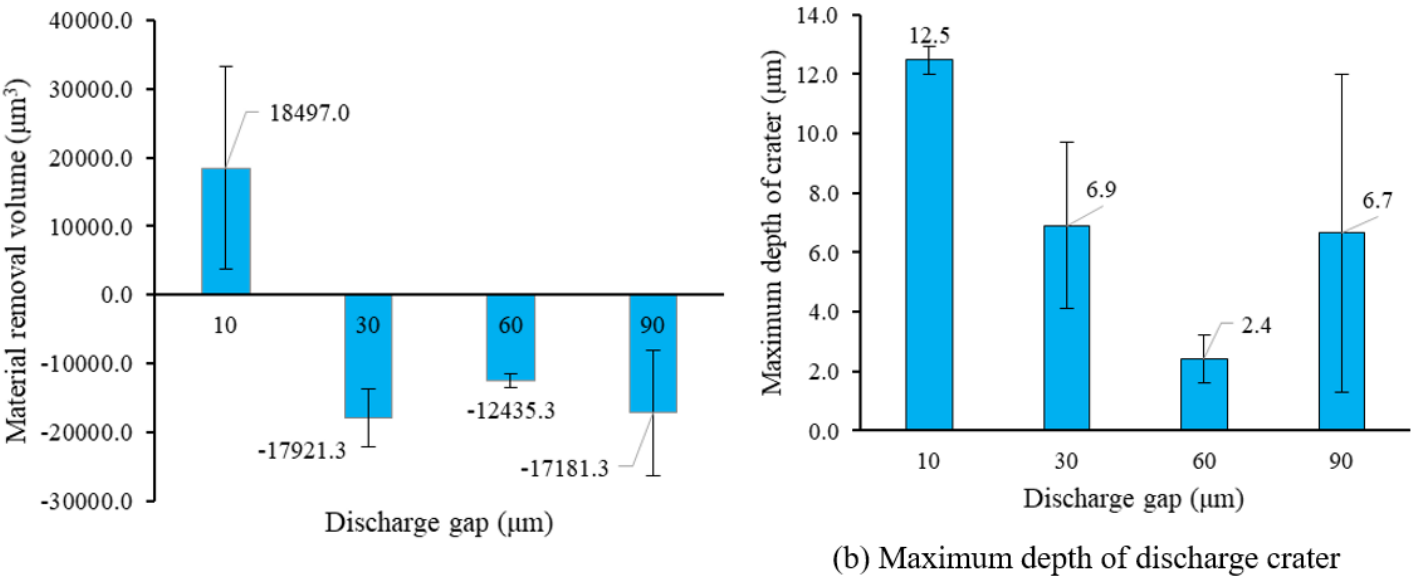

Figure 4

Comparison of discharge crater with different gap widths

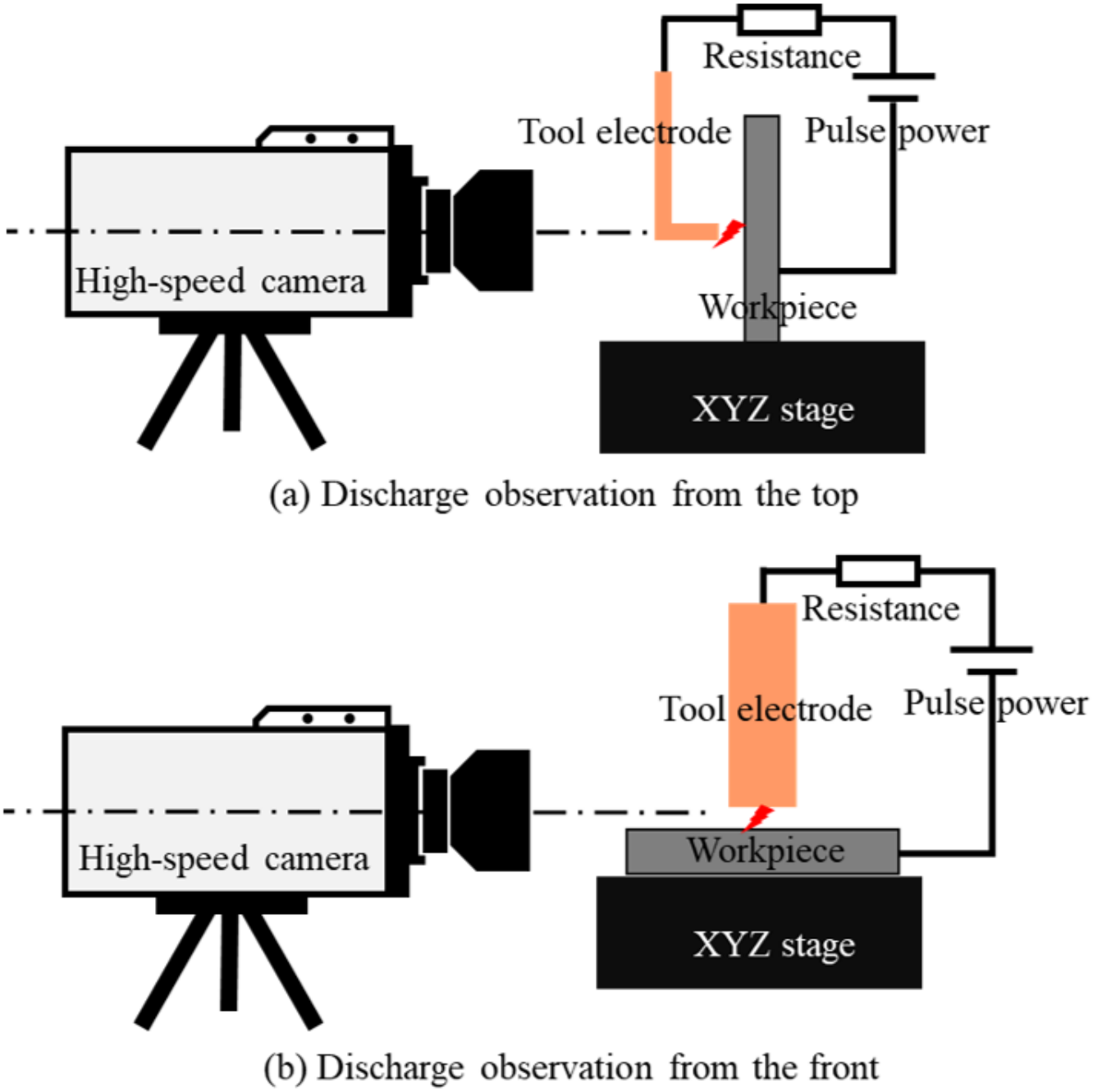

Figure 5

Diagram of discharge process observation

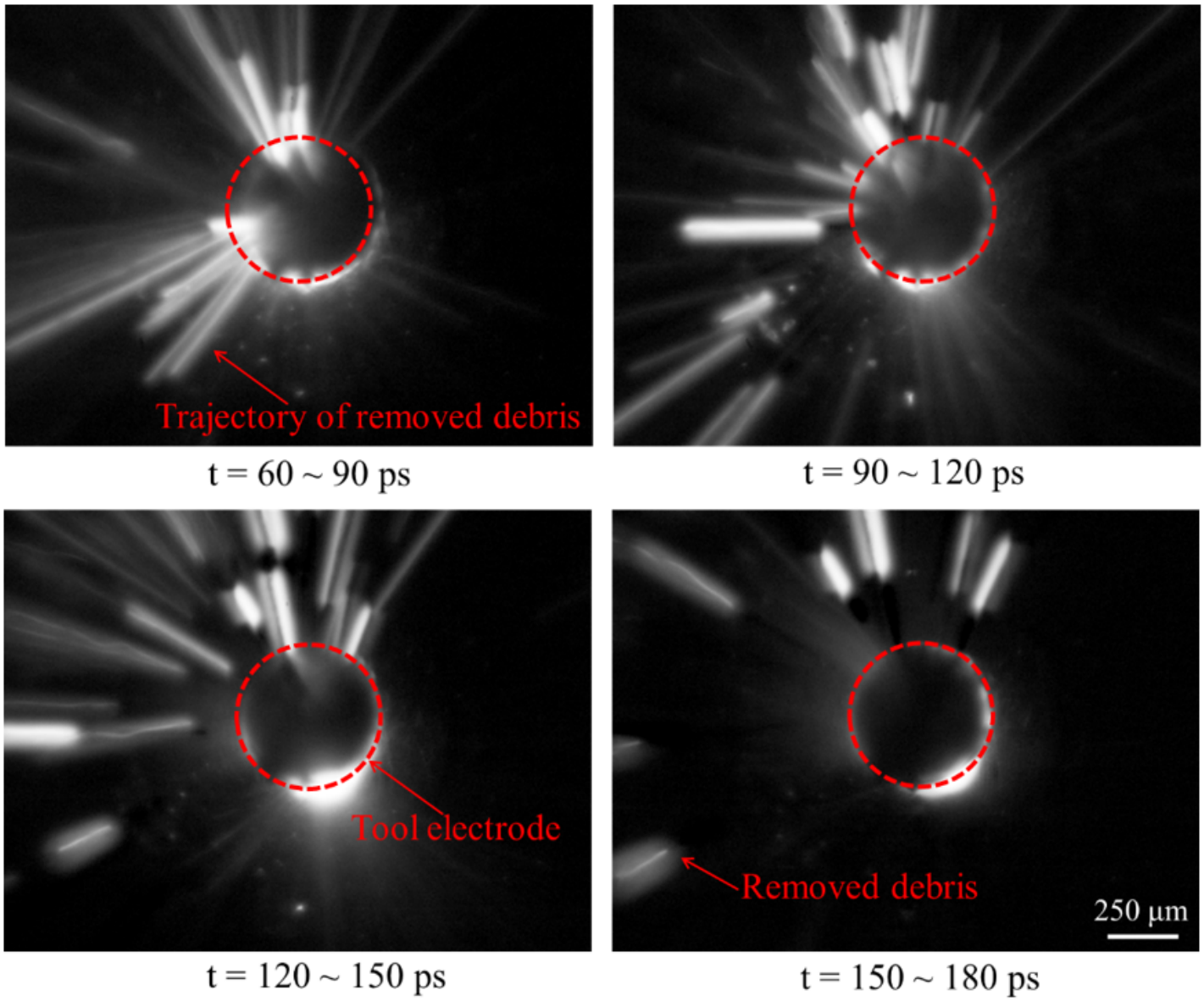

Figure 6

Images of discharge process from top with gap width of 5 μm

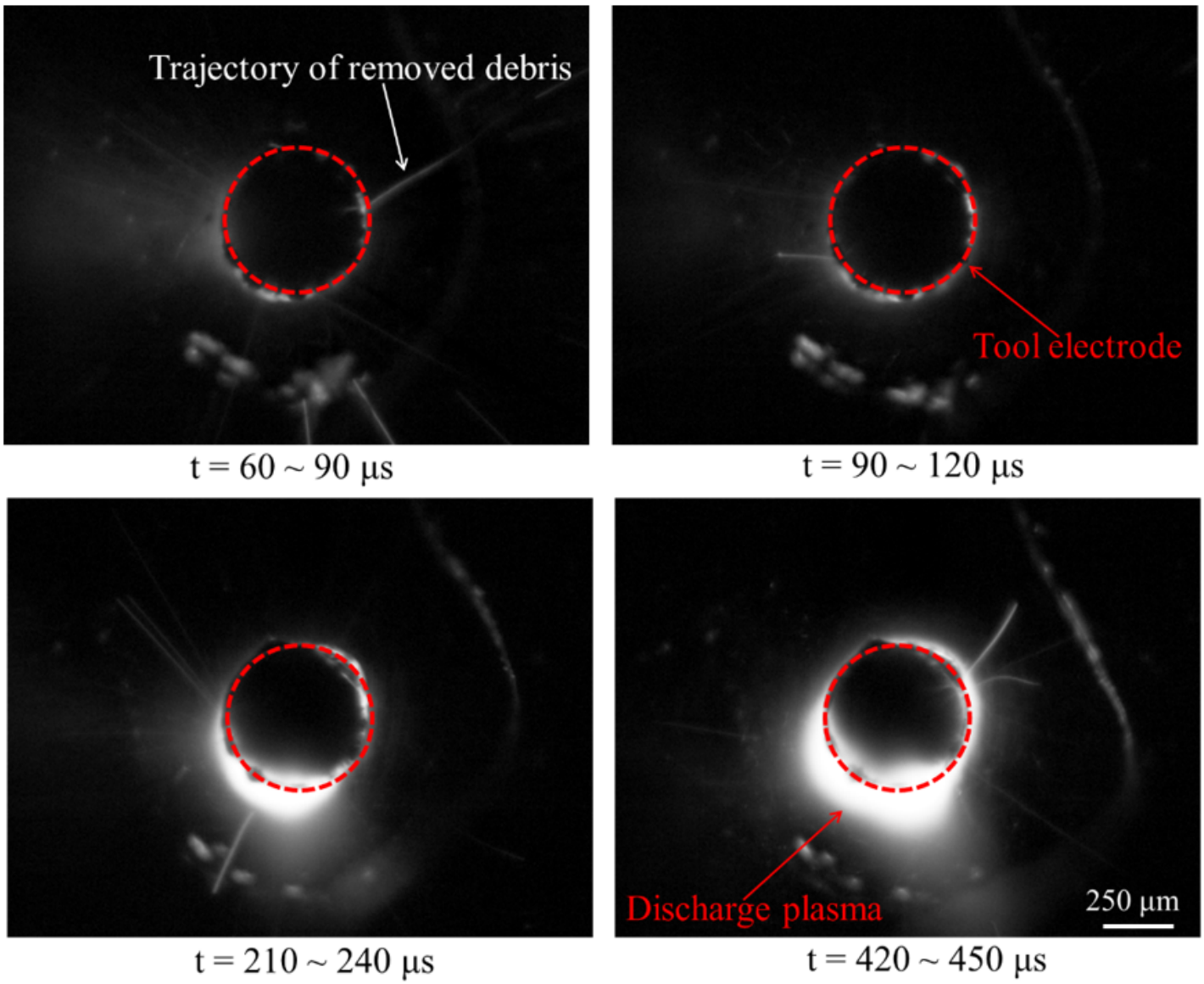

Figure 7

Images of discharge process from top with gap width of 50 μm

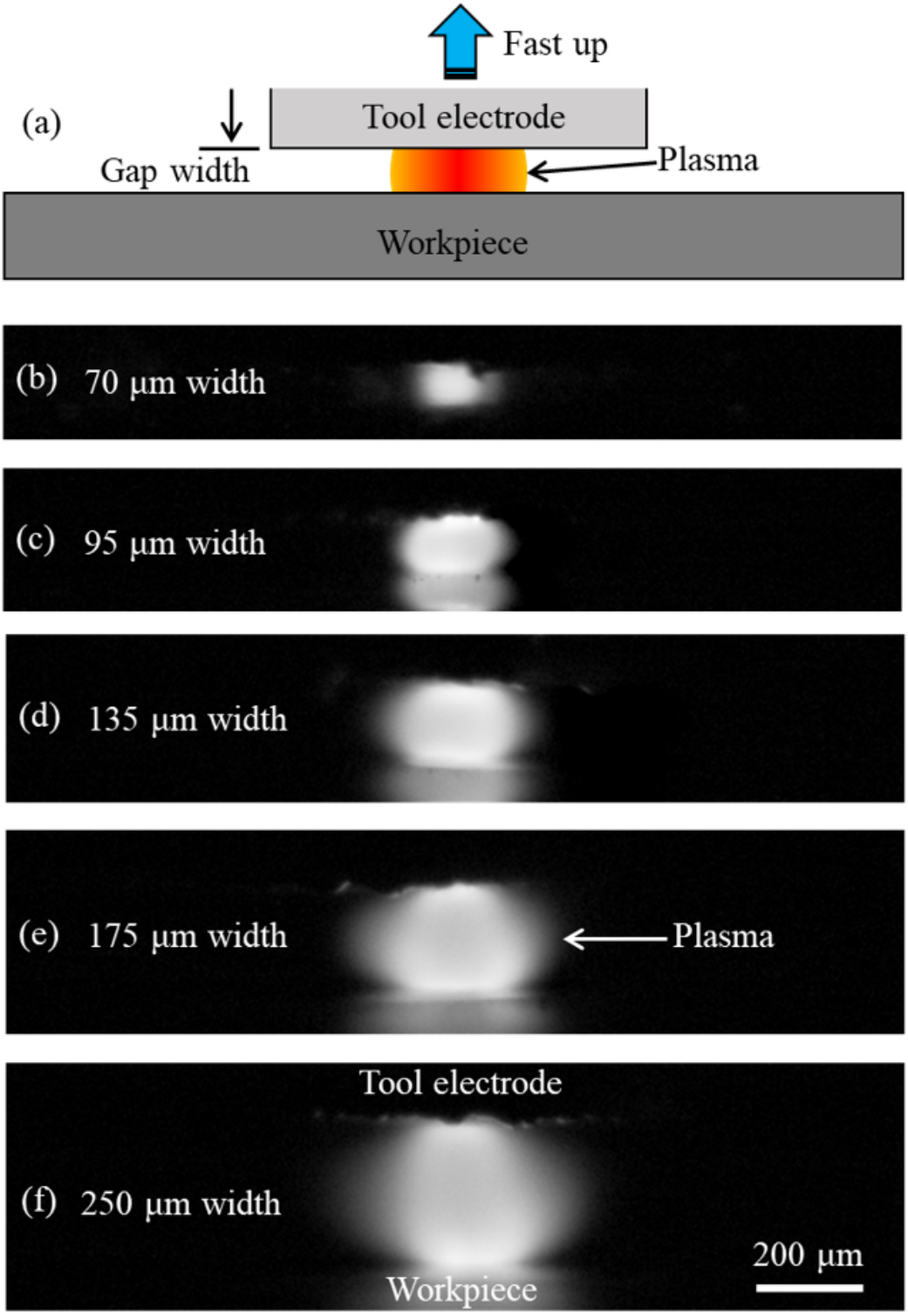

Figure 8

Images of discharge plasma with different gap widths

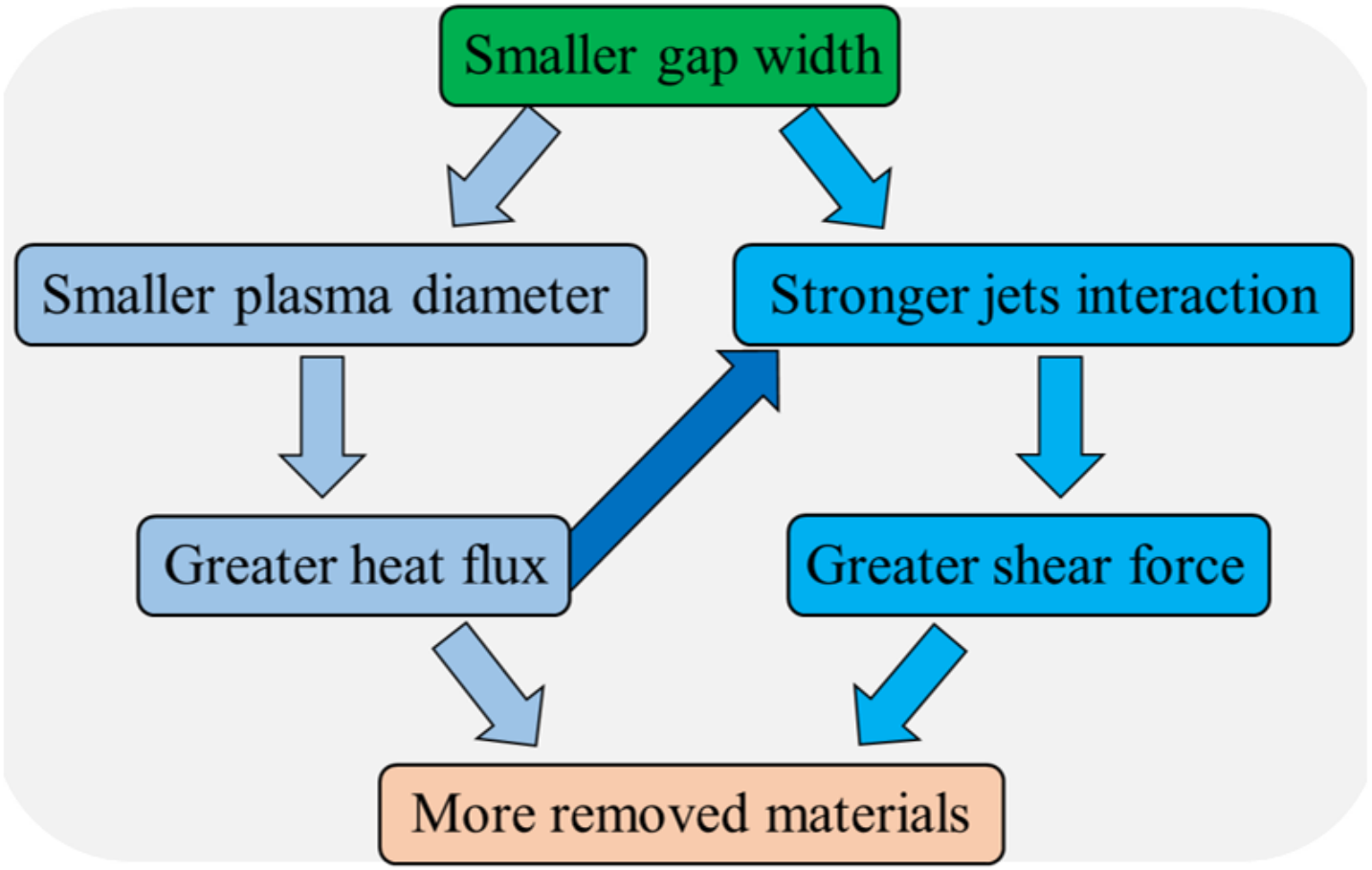

Figure 9

Influence mechanism of discharge gap on material removal in discharge process

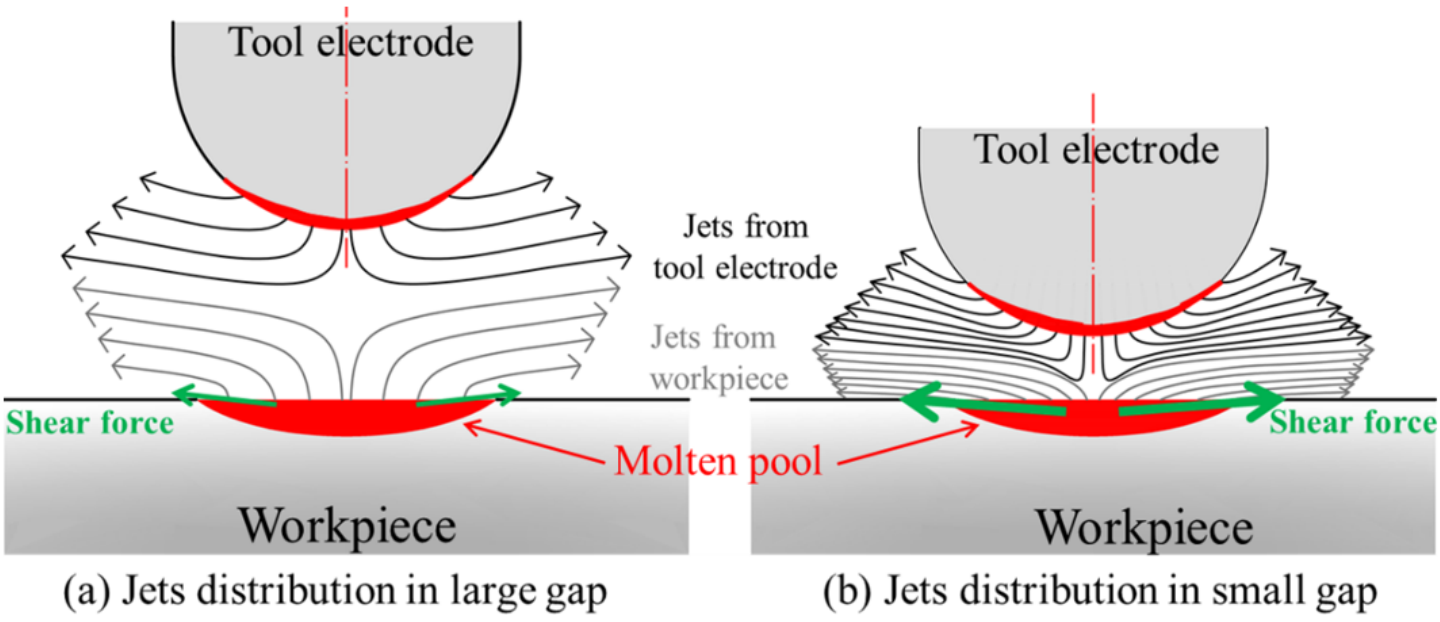

Figure 10

Schematics of interaction of metal vapor jets in gap

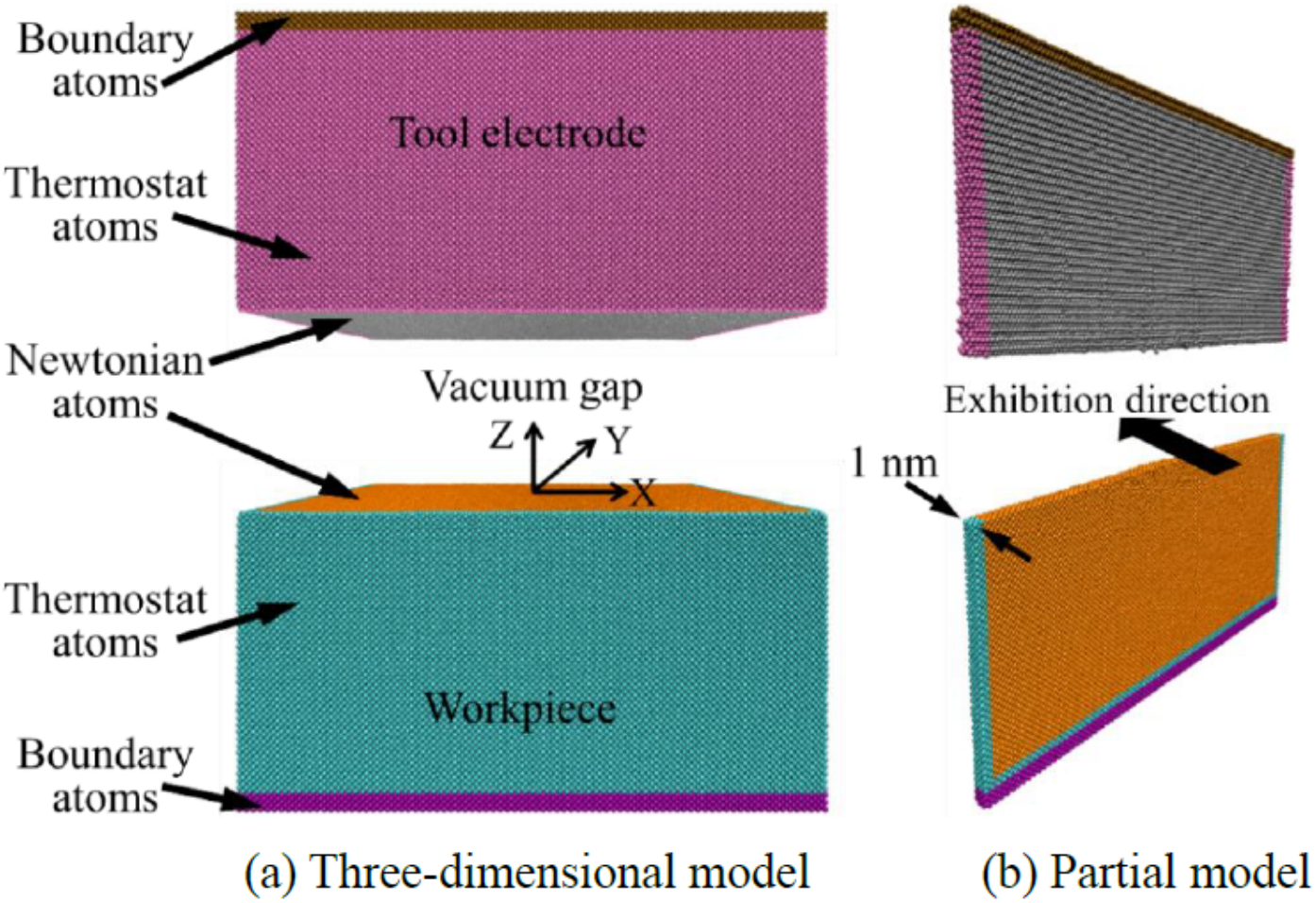

Figure 11

MD simulation model

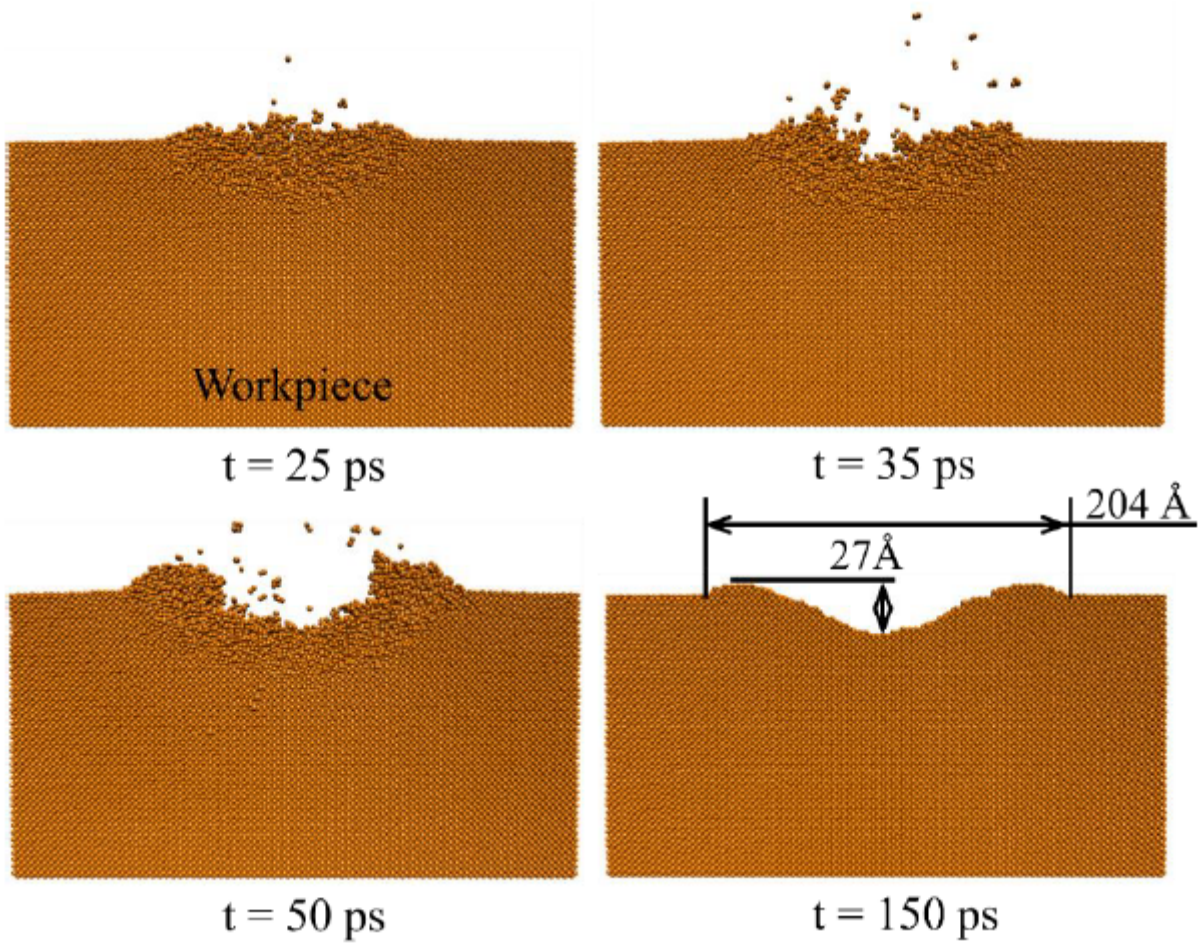

Figure 12

MD simulation of discharge process with heat source diameter of 16 nm

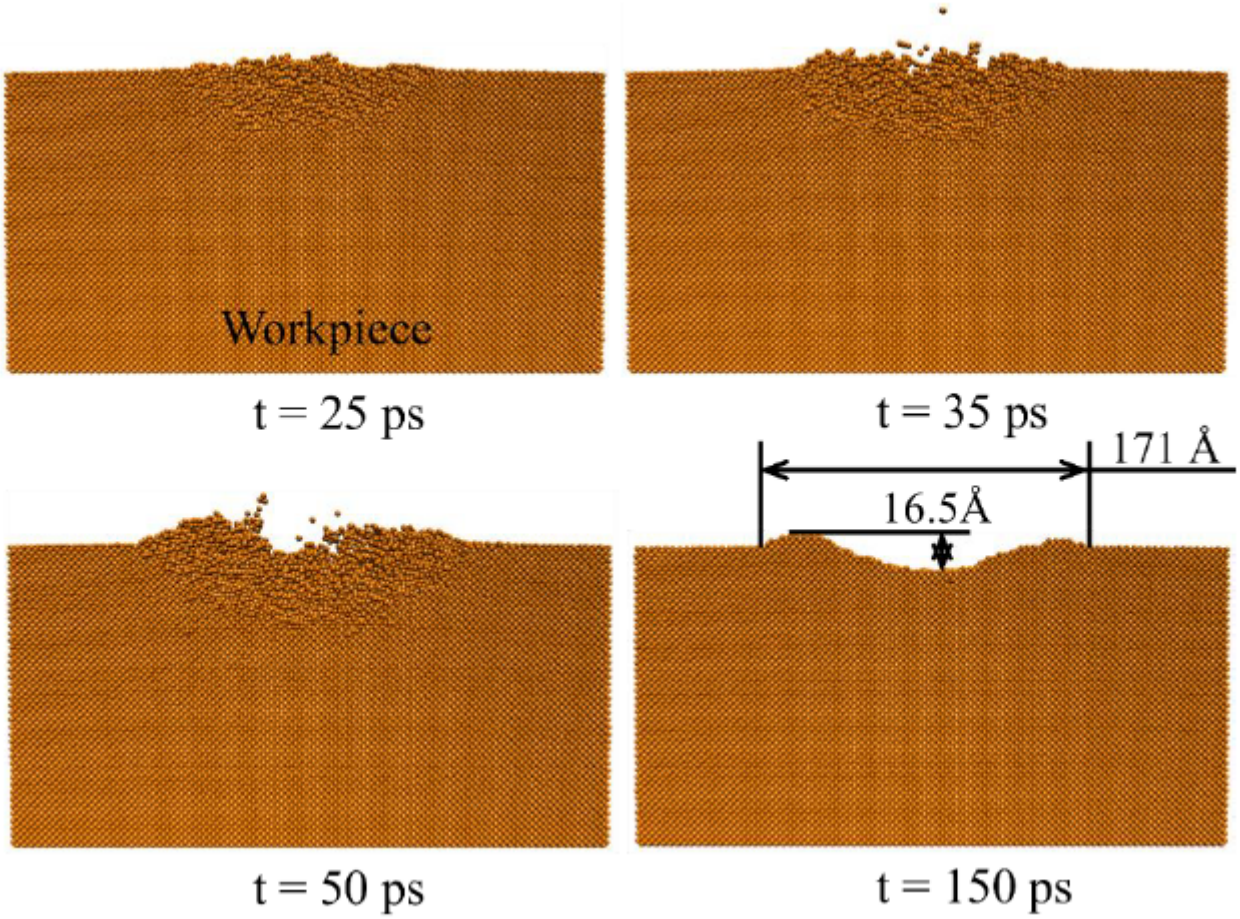

Figure 13

MD simulation of discharge process with heat source diameter of 20 nm

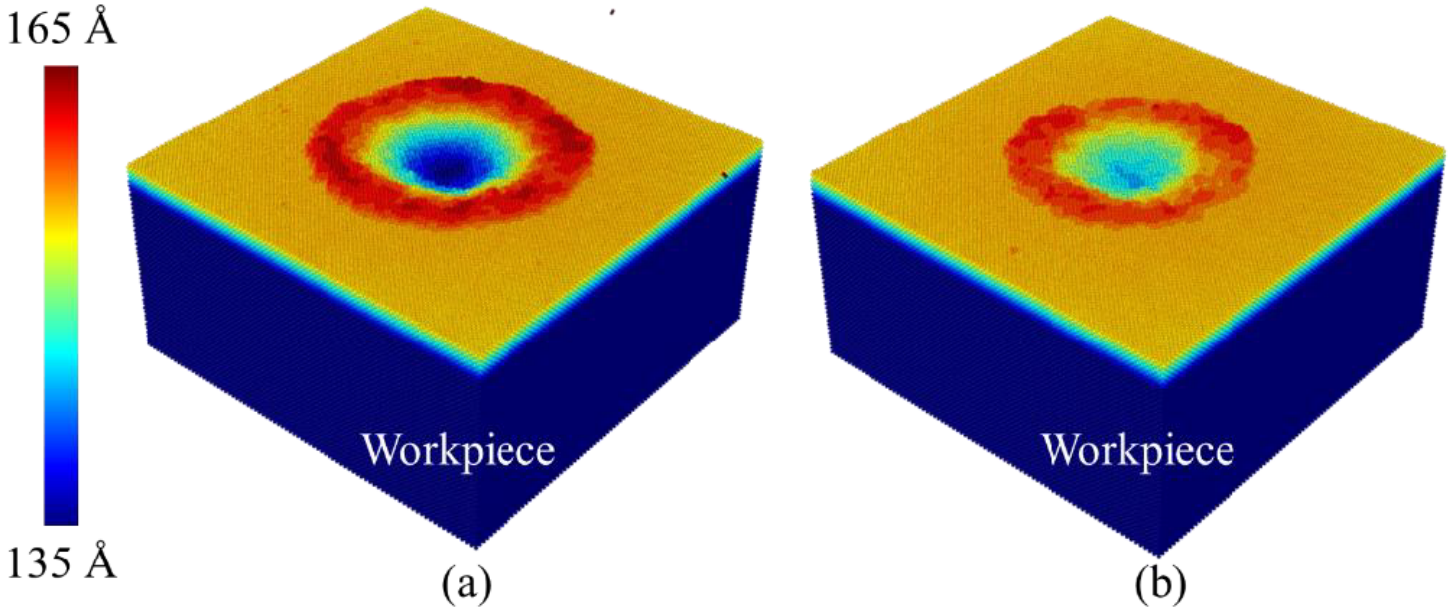

Figure 14

Topography of discharge craters generated in MD simulation with heat source diameter of (a) 16 nm and (b) 20 nm, respectively

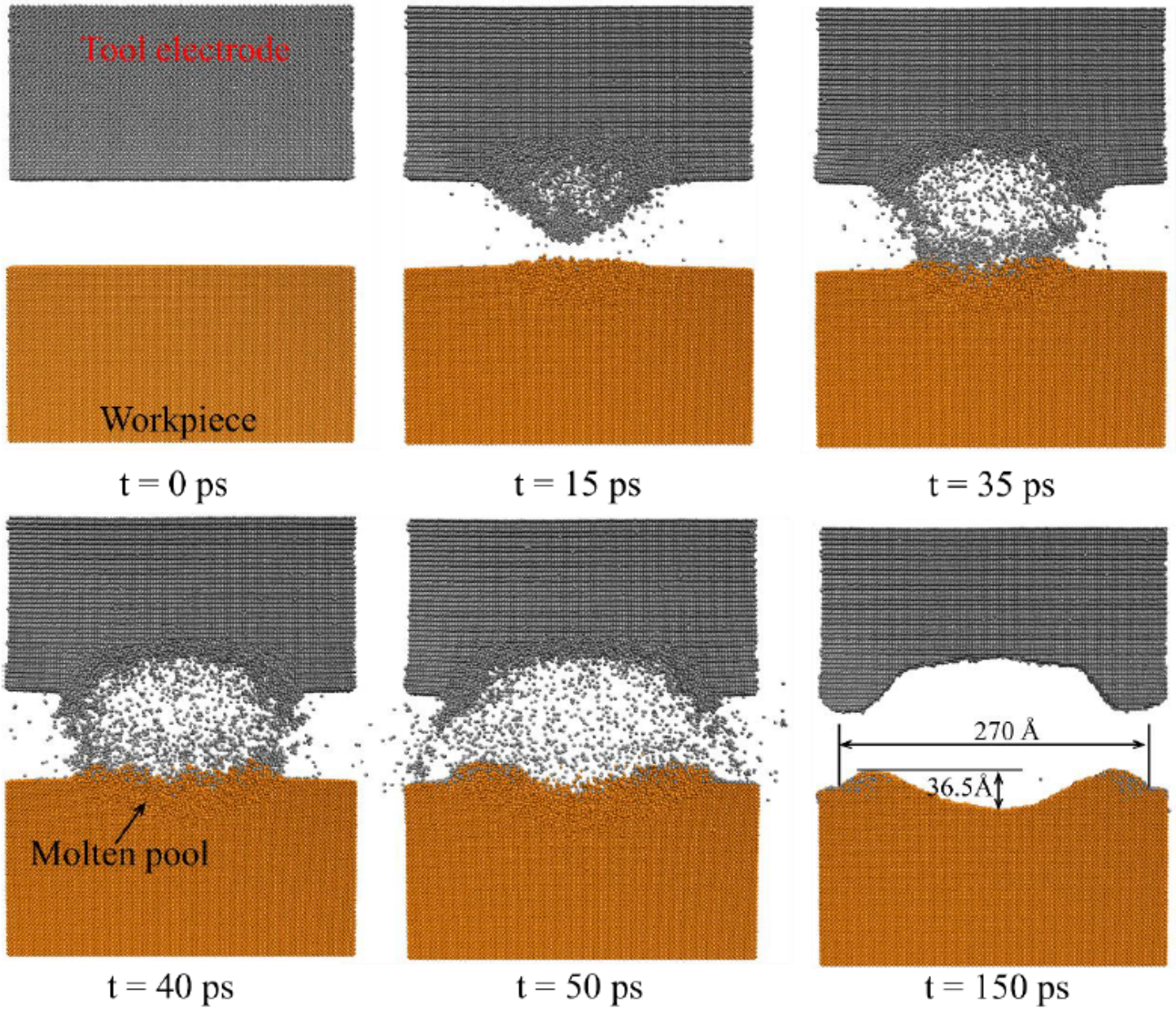

Figure 15

MD simulation of discharge process with gap width of 8 nm

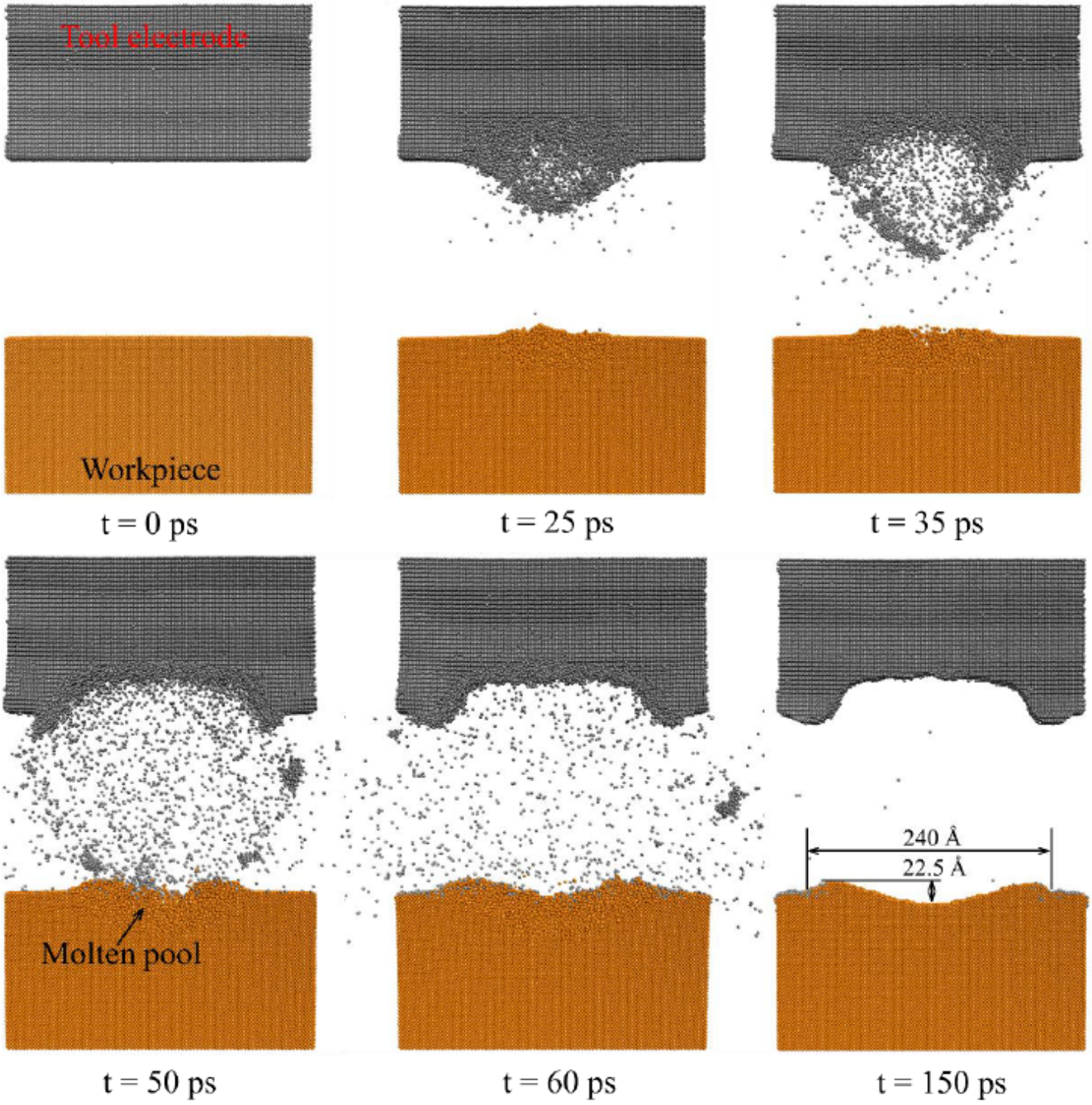

Figure 16

MD simulation of discharge process with gap width of 18 nm

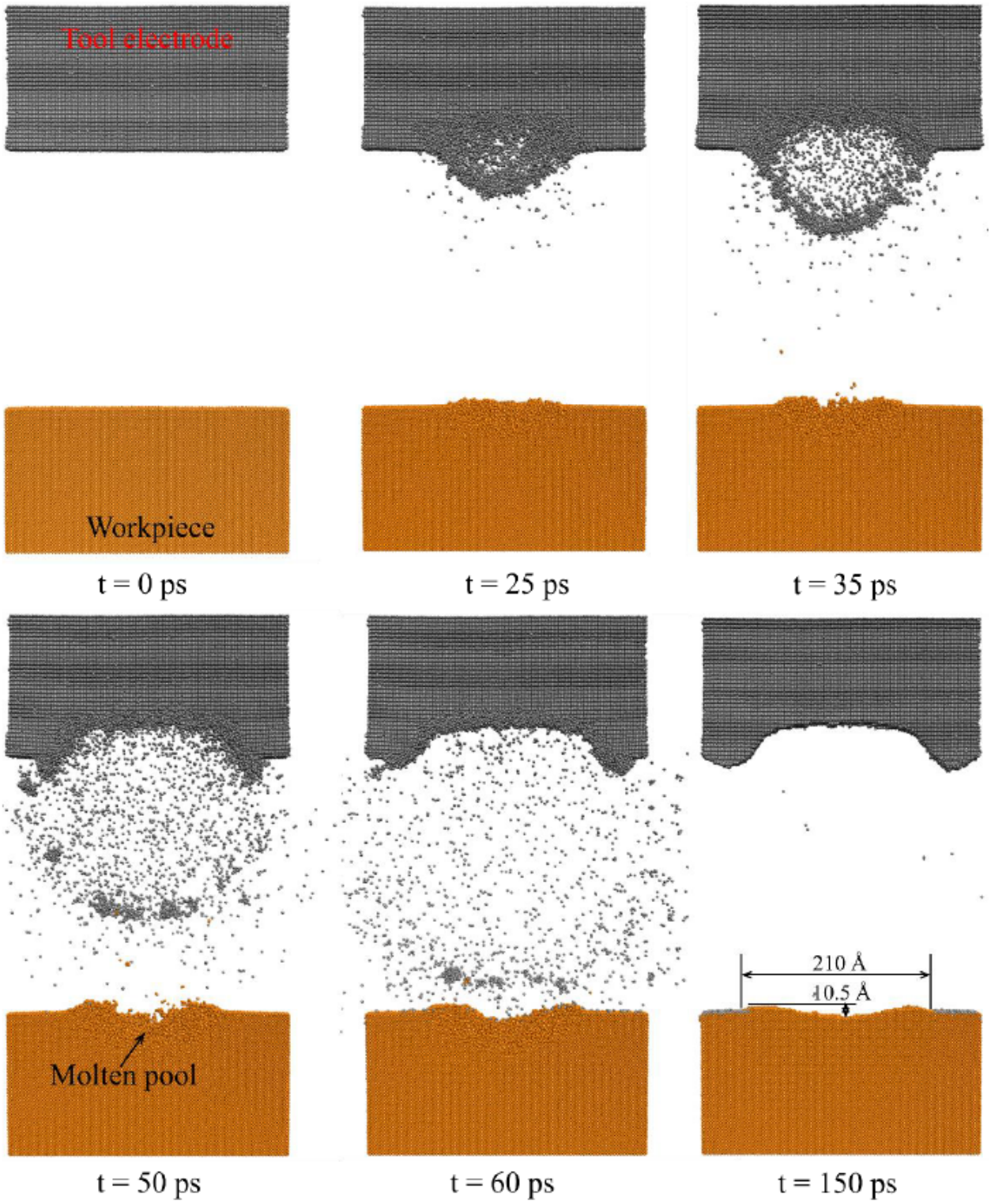

Figure 17

MD simulation of discharge process with gap width of 28 nm

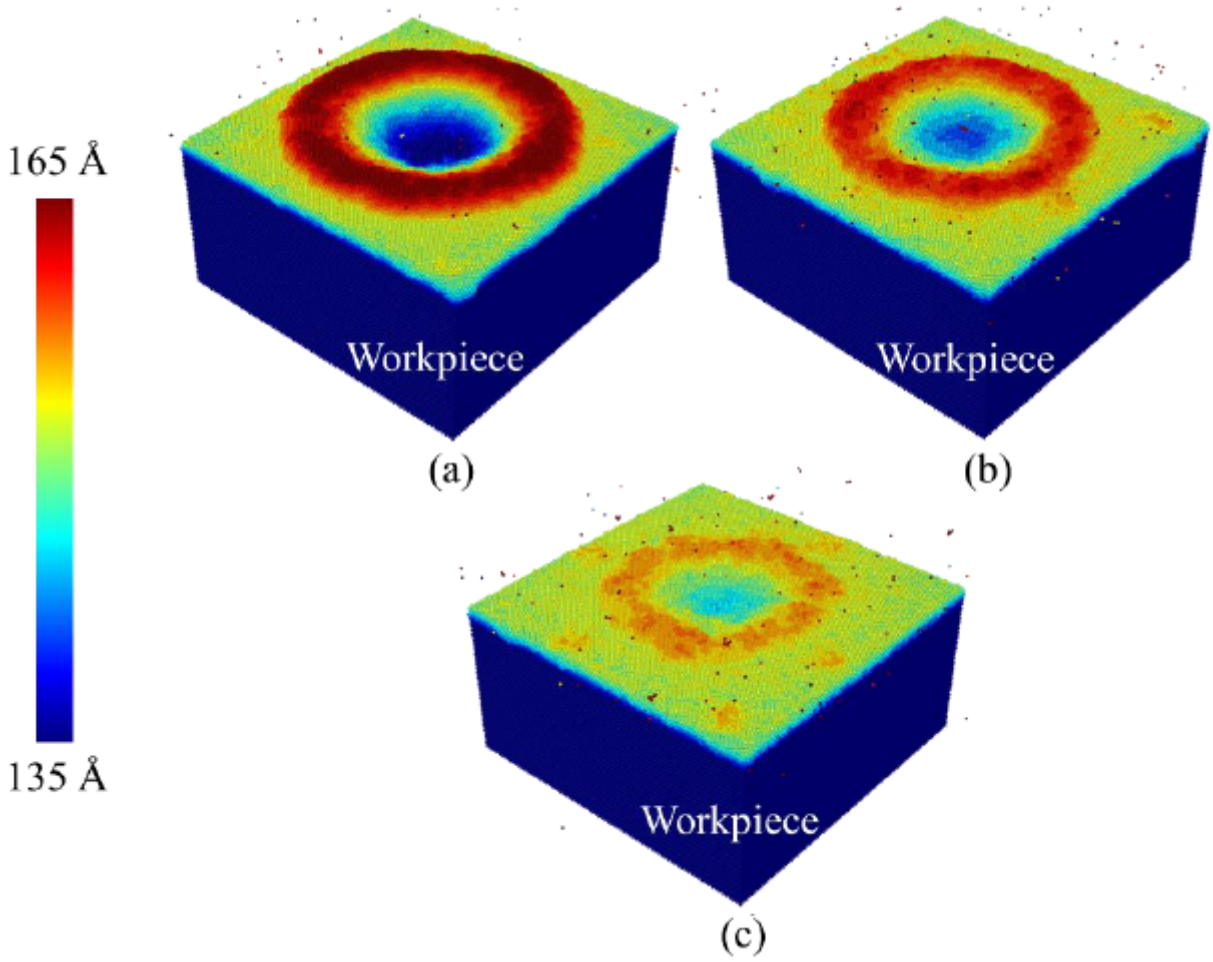

Figure 18

Topography of discharge craters generated in MD simulation with gap width of (a) 8 nm, (b) 18 nm, and (c) 28 nm, respectively

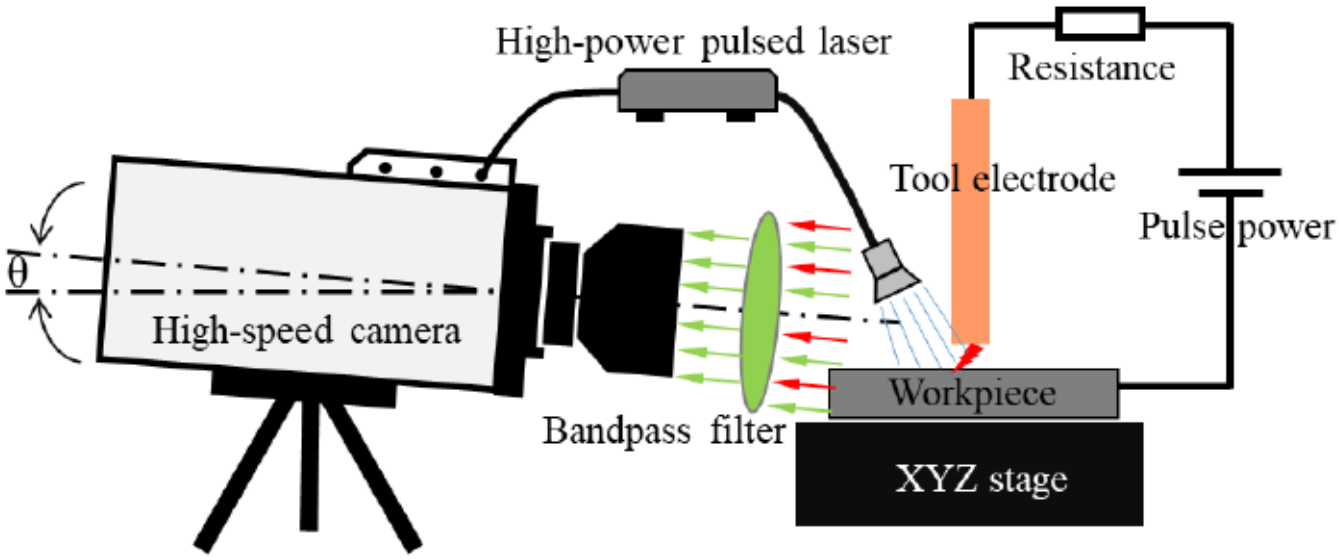

Figure 19

Diagram of melt pool observation

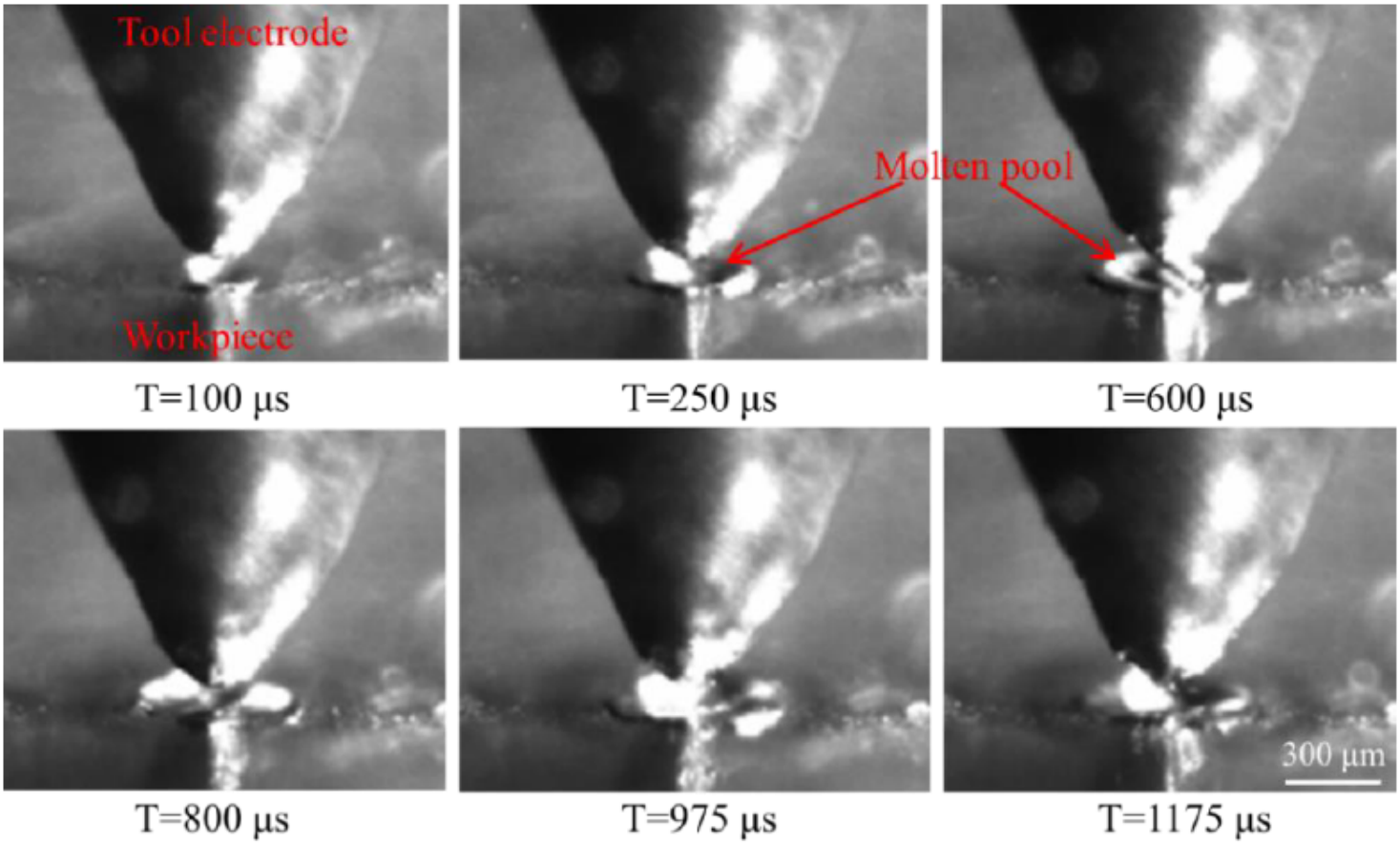

Figure 20

Images of melt pool with gap width of 10 μm

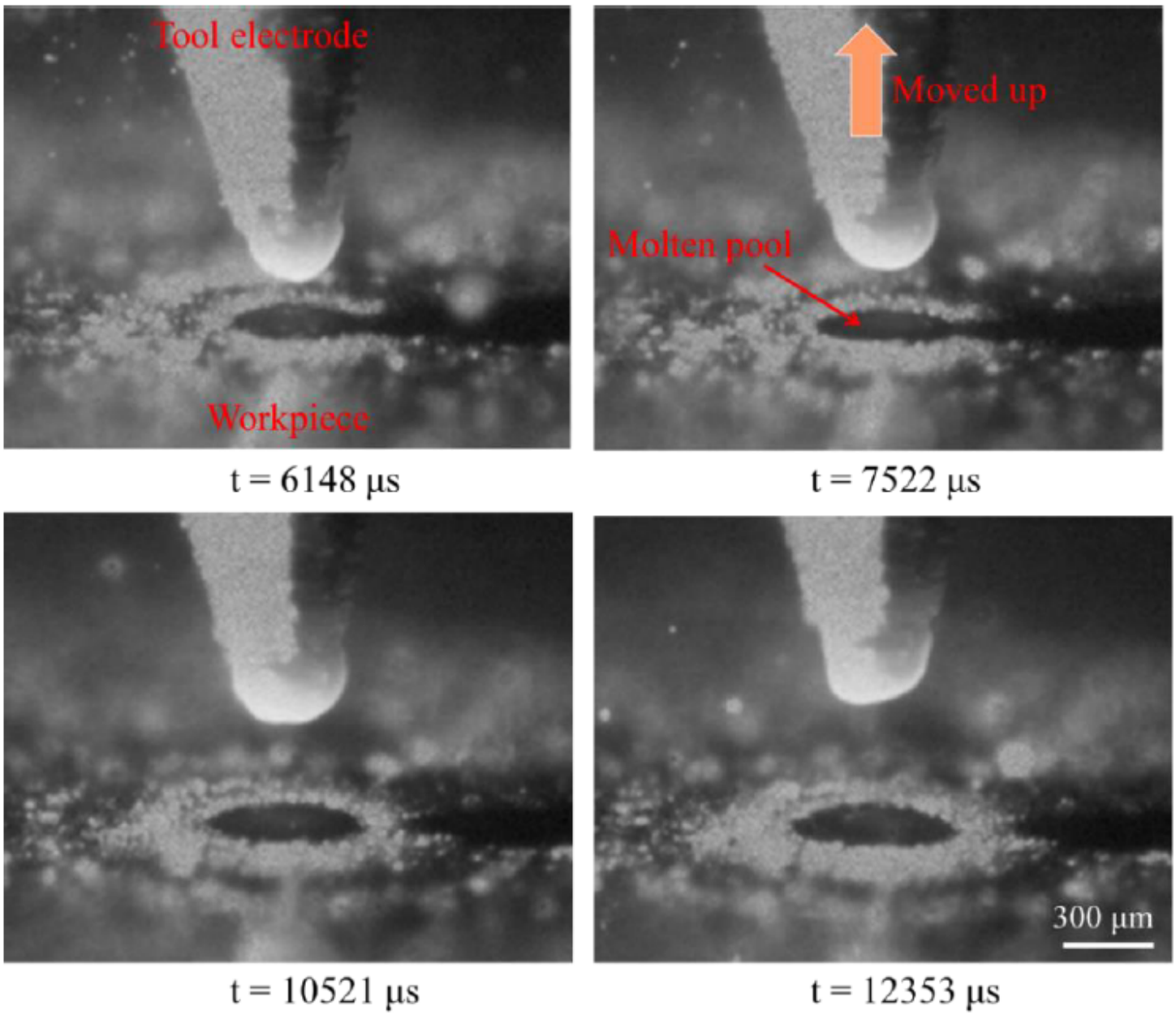

Figure 21

Images of melt pool with large gap width (> 200 μm)

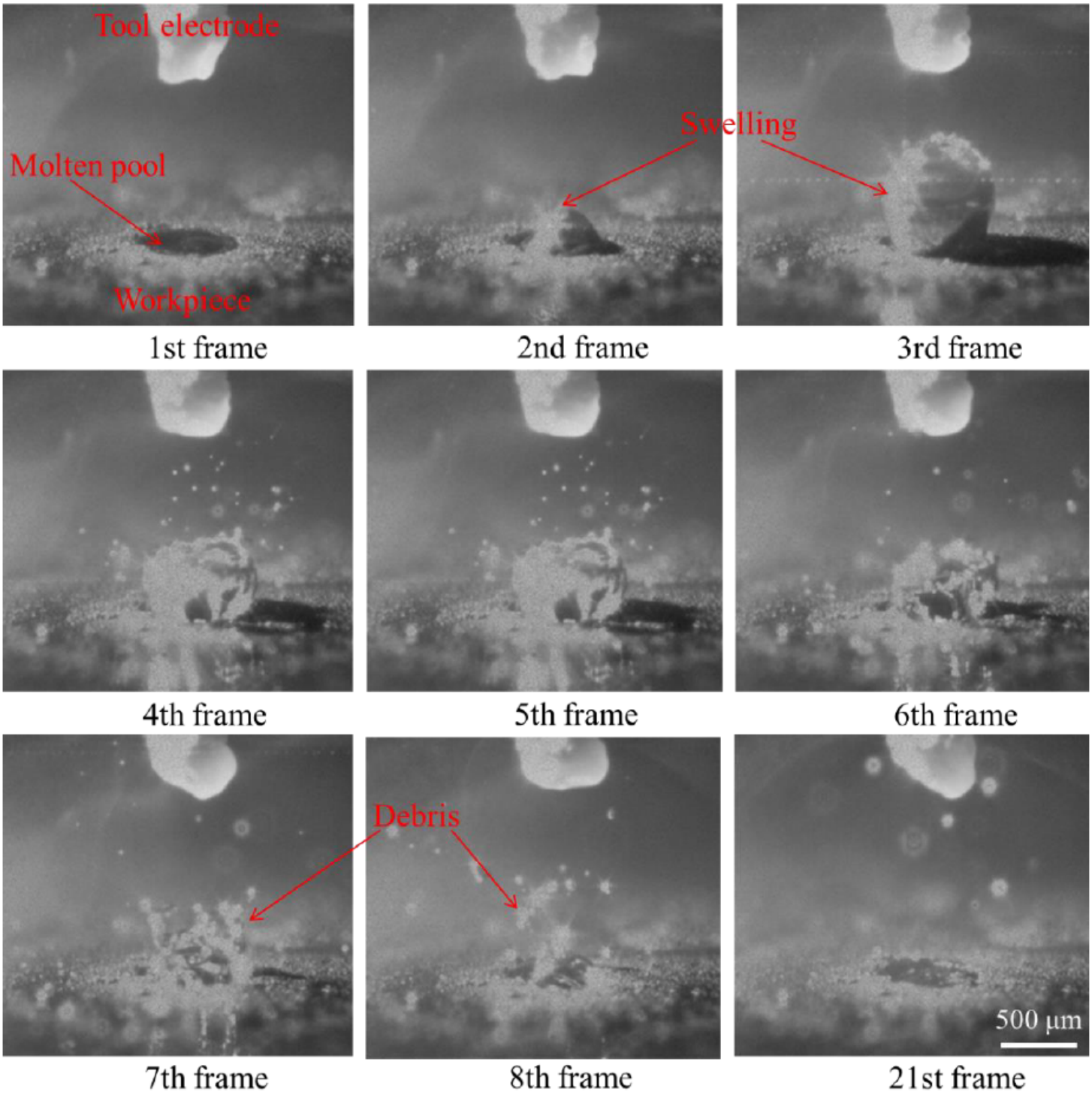

Figure 22

Explosive process of melt pool in discharge

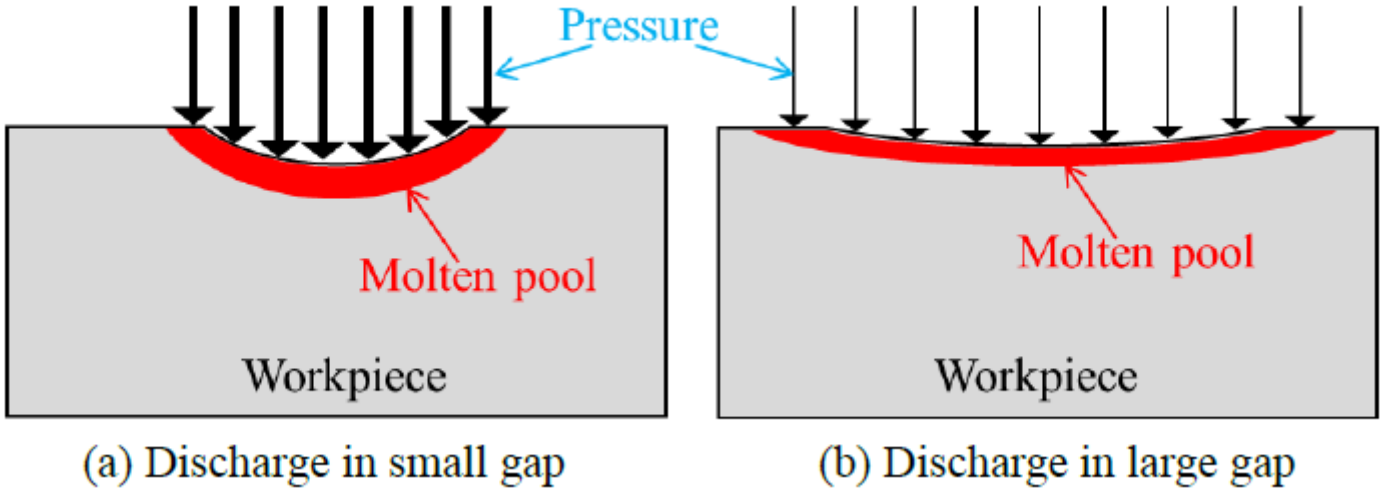

Figure 23

Schematics of gap width influence on melt pool

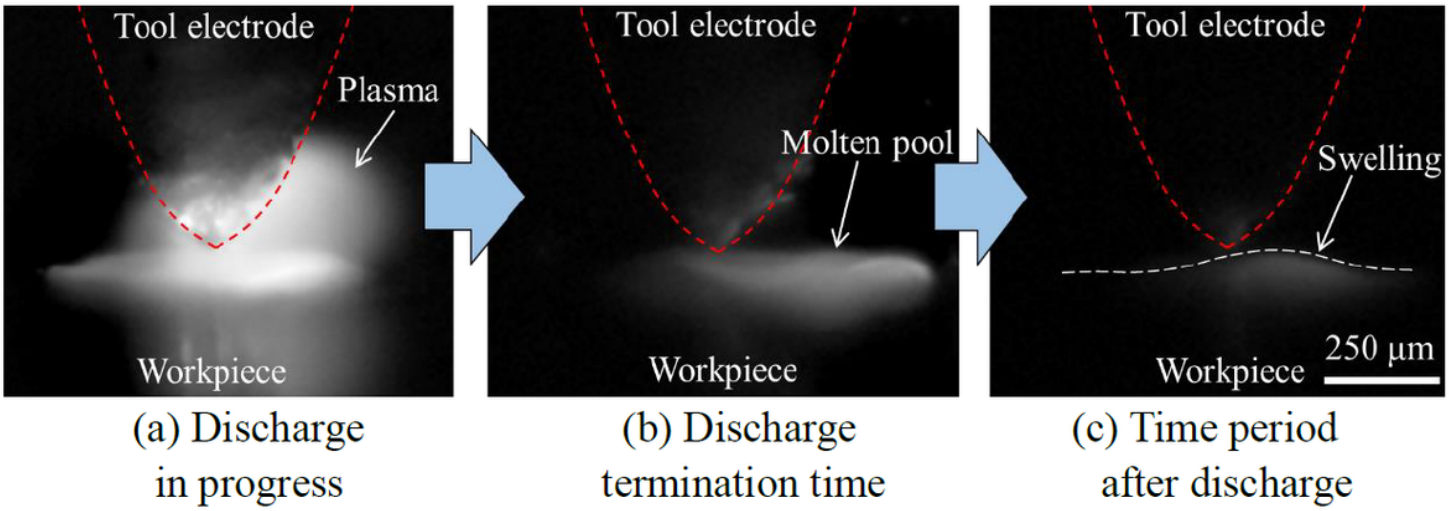

Figure 24

Images of swelling process of melt pool